arXiv:astro-ph/0410494v1 20 Oct 2004

Herbig Ae/Be Stars in nearby OB associations

Jesús Hernández[1,2,3], Nuria Calvet[4,2], Lee Hartmann[4], César Briceño[1,2], Aurora Sicilia-Aguilar[4],
and Perry Berlind[4]

ABSTRACT

We have carried out a study of the early type stars in nearby OB associations spanning an age range of ~ 3 to 16 Myr, with the aim of determining the fraction of stars which belong to the Herbig Ae/Be class. We studied the B, A, and F stars in the nearby (≤ 500 pc) OB associations Upper Scorpius, Perseus OB2, Lacerta OB1, and Orion OB1, with membership determined from Hipparcos data. We also included in our study the early stars in the Trumpler 37 cluster, part of the Cep OB2 association. We obtained spectra for 440 Hipparcos stars in these associations, from which we determined accurate spectral types, visual extinctions, effective temperatures, luminosities and masses, using Hipparcos photometry. Using colors corrected for reddening, we find that the Herbig Ae/Be stars and the Classical Be stars (CBe) occupy clearly different regions in the JHK diagram. Thus, we use the location on the JHK diagram, as well as the presence of emission lines and of strong 12 μm flux relative to the visual to identify the Herbig Ae/Be stars in the associations. We find that the Herbig Ae/Be stars constitute a small fraction of the early type stellar population even in the younger associations. Comparing the data from associations with different ages and assuming that the near-infrared excess in the Herbig Ae/Be stars arises from optically thick dusty inner disks, we determined the evolution of the inner disk frequency with age. We find that the inner disk frequency in the age range 3 - 10 Myr in intermediate mass stars is lower than that in the low mass stars (< 1 M$_\odot$); in particular, it is a factor of ~ 10 lower at ~ 3 Myr. This indicates that the time-scales for disk evolution are much shorter in the intermediate mass stars, which could be a consequence of more efficient mechanisms of inner disk dispersal (viscous evolution, dust growth and settling toward the midplane).

Subject headings: stars: emission-line — stars: pre–main-sequence — stars: Hertzsprung-Russell diagram — open clusters and associations: general

---

[1] Centro de Investigaciones de Astronomía (CIDA), Apartado Postal 264, Mérida 5101-A, Venezuela; Electronic mail: jesush@cida.ve, briceno@cida.ve

[2] Postgrado de Física Fundamental, Universidad de Los Andes (ULA), Mérida 5101-A, Venezuela

[3] Visiting Student, Harvard-Smithsonian Center for Astrophysics

[4] Harvard-Smithsonian Center for Astrophysics, 60 Cambridge, MA 02138, USA, Electronic mail: ncalvet@cfa.harvard.edu, hartmann@cfa.harvard.edu,pberlind@cfa.harvard.edu

1. Introduction

The Herbig Ae/Be stars (HAeBe) are young emission line objects with spectral types B, A, and in a few cases F, in most instances spatially correlated with dark clouds or bright nebulosities (Herbig 1960; Waters & Waelkens 1998; Hernández et al. 2004). The masses of HAeBe range from 2 to 10 $M_\odot$. Like their low mass pre-main-sequence (PMS) counterparts, the T Tauri stars (TTS), these objects become optically visible before reaching the main sequence, so their PMS evolution can be studied in some detail. Stars more massive than 10 $M_\odot$ are expected to spend their whole PMS time as optically obscured objects.

In addition to Hα emission, HAeBe exhibit infrared excesses relative to the photosphere which are attributed to emission from dust in circumstellar accretion disks (Finkenzeller & Mundt 1984; Lorenzetti et al. 1983; Davies et al. 1990; Hillenbrand et al. 1992; van den Ancker et al. 1997; Malfait et al. 1998). Millimetric and submillimetric observations confirm the existence of disks of substantial mass around some of these objects (Blake & Boogert 2004; Fuente et al. 2003; Mannings & Sargent 2000, 1997; Natta et al. 2000, 2001). Most HAeBe exhibit a flux excess in the near infrared (NIR) portion of their spectral energy distributions (SEDs), which has been attributed to emission from an optically thick "wall" at the dust destruction radius, directly heated by the star (Natta et al. 2001; Maheswar, Manoj, & Bhatt 2002; Dullemond et al. 2001; Dullemond & Dominik 2004a; Muzerolle, et al 2004; Muzerolle, Calvet, Hartmann, & D'Alessio 2003b).

Studies of the circumstellar environments of HAeBe suggest that these objects are progenitors the stars surrounded by debris disks (e.g, β Pictoris, Vega-like stars), which could be sites of planet formation (Natta et al. 2000; Lagrange, Backman, & Artymowicz 2000). However, long standing questions about how and when the transition between HAeBe and Vega-like stars occurs have yet to be answered. Observations of the numbers of young intermediate mass stars surrounded by optically thick inner disks in samples of different ages could be used as a first step toward answering these questions. Roughly coeval stellar groups are ideal to study since uncertainties in properties like distances and ages are minimized.

OB associations are defined as stellar groups with significant populations of intermediate mass stars and with stellar mass density less than 0.1 $M_\odot/pc^3$ (Brown et al. 1999b). Ages derived from Hertzsprung-Russell diagrams (HRD) indicate that they are young (e.g, Blaauw 1964). For this reason, OB associations are excellent for studying young stellar objects covering a complete range of mass (e.g. Preibisch et al. 2002). Moreover, by studying OB associations with different ages, we can analyze the temporal evolution of the processes characterizing the early history of their stars.

An important but difficult aspect of studying OB associations is the identification of their members. OB associations have small internal velocity dispersions, so the streaming motion of the stellar group, in combination with the solar motion, is reflected as a motion of their members toward a convergent point on the sky (e.g., Brown et al. 1999a; de Zeeuw et al. 1999). Thus, membership can be established by studying the kinematic properties of the group (proper motions, parallaxes, radial velocities). Nearby associations cover large regions in the sky, which in the past limited the astrometric membership determination to the bright stars (V $\leq$ 6 mag). Photometric studies could add fainter members to the associations, but this membership determinations were less reliable due to several factors as, for instance, undetected duplicity, spread of distances within the association, photometric variability, and interlopers. The publication of positions, proper motions and trigonometric parallaxes for $\sim$120000 stars in the Hipparcos Catalog (Esa 1997) has significantly improved the situation, enabling astrometric studies down to its limiting magnitude, V$\sim$12.

Using Hipparcos measurements, de Zeeuw et al. (1999) made a comprehensive census of the stellar content of the OB associations within 1 Kpc from the sun. Members of each association were identified using two methods. The first method is a modification of the classical convergent point method (Brown 1950) detailed by de Bruijne (1999); the second uses the positions, parallaxes and proper motions to define members using probability distributions in the velocity space (Hoogerwerf & Aguilar 1999). The combination of these methods gives reliable memberships of stars in 12 young stellar groups. However, since some groups are beyond 500 pc, where the Hipparcos parallaxes are no longer useful, or have unfavorable kinematics, 10 associations studied by de Zeeuw et al. (1999) do not show astrometric evidence for a moving group and their results are inconclusive. One of these associations with unfavorable kinematics is Orion OB1, which has a motion mostly directed radially away from the Sun. Nonetheless, the Hipparcos data of Ori OB1 was analyzed carefully by Brown et al. (1999b), who found a relation based on proper motions which characterizes approximately the members of this association (see §2.2). The resulting set of stars selected by this relation overlaps in 96% with the photometric members given by Brown, de Geus, & de Zeeuw (1994).

In this contribution we explore the frequency of HAeBe in three associations with different ages (Upper Scorpius, Perseus OB2, and Lacerta OB1) with members selected from de Zeeuw et al. (1999). In addition, we study the Orion OB1 association, which was divided in 2 sub-association with different ages and distances. We complement our studies by analyzing the NIR properties of the early stars in Trumpler 37 from Contreras et al. (2002). Details of the selection and the observation of each sample is described in §2. In our entire sample, more than 82% of the spectral types published by Hipparcos are from the SIMBAD[1] data-base, with references labeled as miscellaneous; the other 18% are from the Michigan catalogue for the HD stars (Houk 1982; Houk & Smith-Moore 1988). We obtained spectra for all the stars in our sample and reclassified them using the classification scheme described in Hernández et al. (2004), to obtain an homogeneous spectral typing scheme for all the objects in the associations. Details of the classification scheme are in §3.1, where we also calculate the visual extinction for the objects and describe the identification and measurement of the emission lines present in the spectra. We analyze the NIR excess of the members of each group in §3.2. We estimate distances from both astrometric and photometric data in §3.3, and a HRD is given for each association in §3.4. A census of HAeBe, based on observational properties characteristic of the presence of disks (emission at Hα, NIR excesses and IRAS fluxes) is described in §4, and the disk frequency is discussed on §5. Finally, we summarize the most important aspects of this work in §6.

---

[1] SIMBAD, Centre de Données astronomiques de Strasbourg: http://simbad.u-strasbg.fr/sim-fid.pl

2. Selection of the sample and observations

Table 1 lists properties of the associations studied in this contribution. Our total sample include 440 Hipparcos stars distributed in 3 OB associations (§2.1), with astrometric membership determined by de Zeeuw et al. (1999), and the Orion OB1 association, for which we have determined membership combining astrometric and photometric data (§2.2).

2.1. Upper Scorpius, Perseus OB2 and Lacerta OB1 sample

Using the census of nearby OB associations made by de Zeeuw et al. (1999), we selected young associations with estimated ages < 20 Myr and within 500 pc from the sun, since the uncertainty in the Hipparcos parallaxes beyond 500 pc is generally larger than 50%. We also required the associations to be within the declination limit of the telescope used in this work ($\delta > -35°$, see §2.3). With this criteria we selected the OB associations Upper Scorpius (US), Perseus OB2 (Per OB2), and Lacerta OB1 (Lac OB1). Columns 2, 3, 4 of Table 1 give the distances, the ages, and the number of stars for each association, respectively (de Zeeuw et al. 1999). Column 5 of this table gives the number of stars observed for each one of these three associations. Other information in this table is discussed below.

2.2. Orion OB1 sample

As we said previously, the association Orion OB1 has unfavorable kinematics, so the membership determination method from de Zeeuw et al. (1999) is not useful. However, Brown et al. (1999b) and Brown, de Geus, & de Zeeuw (1994) studied in detail the brighter population of this association giving several criteria to find members belonging to Ori OB1. These criteria are applied in this section to create our sample.

We defined a region of 180 square degrees in Orion OB1 defined by limits in right ascension $5.0h < \alpha < 6.0h$ and declination $-6° < \delta < 6°$. There are 733 Hipparcos stars in this region. Since the motion of the Ori OB1 association is mostly directed radially away from the Sun, the expected intrinsic proper motions in right ascension and declination, μ_α and μ_δ, have to be small and comparable to measurement errors. So, we rejected stars with a relative large intrinsic proper motion by applying the criteria defined by Brown et al. (1999b),

$$(\mu_\alpha cos(\delta) - 0.44)^2 + (\mu_\delta + 0.65)^2 \leq 25 \tag{1}$$

Where the proper motions are in milli-arcsecond per year (mas/yr)

This method provides a rough selection of members in Orion OB1. From the 282 stars selected by this criterion, we rejected 14 stars because they have negative parallaxes. Another 4 stars were rejected because they are clearly foreground stars with parallaxes larger than 7 mas and corresponding to distances smaller than 140 pc. In addition, using photometry from the Hipparcos catalog, we applied a photometric criterion in the B-V vs V color-magnitude diagram, selecting stars located above or on the zero age main sequence (ZAMS; Cox 2000) and with B-V color ¡ 1.2 in order to avoid highly embedded objects or intrinsically red stars (K and M). The final set of candidates include 245 objects, of which 92% were observed spectroscopically (see Table 1).

Four subgroups of Ori OB1 with differences in ages and distances (1a, 1b, 1c and 1d) were identified by Blaauw (1964). These subgroups were largely analyzed in later studies (e.g., Warren & Hesser 1977a,b; Genzel & Stutzki 1989; Brown, de Geus, & de Zeeuw 1994). Particularly, Brown, de Geus, & de Zeeuw (1994) determined ages (1a: 11.4 ± 1.9 Myr; 1b: 1.7 ± 1.1 Myr; 1c: 4.6 ± 2.0 Myr) and distances (1a: 380 ± 90 pc, 1b: 360 ± 70 pc; 1c: 400 ± 90 pc) based on the photometric properties of each subgroup. Brown et al. (1999b) improved the estimate of distances based on Hipparcos parallaxes (1a: 336 ± 16 pc, 1b: 439 ± 33 pc; 1c: 462 ± 36 pc). The distance of the youngest subgroup Ori OB1d (< 1Myr), located at the Orion Nebula Cluster (ONC), was undetermined due to the small number of stars in the Brown et al. (1999b) study.

Figure 1 shows stars in the Orion OB1 association overlaid on a map of integrated ^{13}CO emissivity from Bally, Stark, Wilson, & Langer (1987) (gray scale) and isocontours of galactic extinction for $A_V = 1, 2, 3$ and 4, from Schlegel, Finkbeiner, & Davis (1998). We plot the boundaries from Warren & Hesser (1977a) between the subgroups 1a, 1b, and 1c. Due to the similarities in the ages and distances of the sub-associations OB1b and OB1c, we have joined these sub-associations into one (labeled as OB1bc). Most of the stars in OB1bc are spatially related with dust or gas. There is a subset of 17 stars in the OB1a sub-association which is also spatially correlated with dust and gas (see Figure 1); we assumed that this subset belongs to OB1bc instead of OB1a. A Kolmogorov-Smirnov test based on Hipparcos parallaxes supports this assumption. This test shows that the significance level is 10% higher when the parallaxes of this subset are compared to the parallaxes of OB1b than when they are compared to the parallaxes of the remainder OB1a stars. The last two rows in Table 1 give information about the subgroups in Ori OB1.

2.3. Observations

We obtained low-dispersion spectra for the stars selected as discussed in §2.1 and §2.2 during 2000 and 2003 using the 1.5 meter telescope of the Whipple Observatory with the FAST Spectrograph (Fabricant et al. 1998), equipped with the Loral 512 × 2688 CCD. The spectrograph was set up in the standard configuration used for “FAST COMBO” projects, a 300 groove mm^{-1} grating and a 3” wide slit. This combination offers 3400 Å of spectral coverage centered at 5500 Å, with a resolution of 6 Å. The spectra were reduced at the CfA using software developed specifically for FAST COMBO observations. All individual spectra were wavelength calibrated and combined using standard IRAF routines [2]. The exposure time range from 0.2 to 180 seconds. Signal-to-noise ratio (SNR) of our spectra are typically $\gtrsim 20$ at the central wavelength region of the spectra. The standard stars used in our spectra classification scheme were observed with the same instrumental configuration used for the Hipparcos stars.

3. Analysis of the observations

Table 2 compiles properties derived from our observations. Column 1 and 2 show the Hipparcos number and other name of the stars. Spectral types and reddening (A_V), with their respective errors, are in columns 3, 4, 5, and 6 (see §3.1). The 2MASS colors used in §3.2 are shown in columns 7, 8 and 9. The effective temperature ($T_{\rm eff}$), luminosity and mass calculated in §3.4 are given in the last three columns.

3.1. Spectral analysis and reddening estimates

We classified ours objects following the spectral classification scheme of Hernández et al. (2004), which is optimized for the FAST wavelength range and is defined for stars with spectral types in the range from O to early G stars. The scheme is based on 33 spectral indices sensitive to changes in $T_{\rm eff}$ but insensitive to reddening, stellar rotation, luminosity class and signal-to-noise ratio. This scheme is designed to largely avoid problems caused by non-photospheric contributions (mostly due to material surrounding the star). We achieve this by requiring that the various spectral types calculated from each index agree with the others; wildly discrepant values are rejected, and a weighted mean spectral type is obtained. In columns 3 and 4 of Table 2, the spectral type and its respective error is show for each star. This error has two contributions, the error from the fit of each index to the standard main sequence, and the error in the measurement of each index (Hernández et al. 2004)

We measured the equivalent width (EW_λ) of Hα and of the most prominent emission lines using the task *splot* in the IRAF spectra reduction package *noao.onedspec*. In those lines with emission and absorption components, the EW_λ is referred to the emission contribution. These emission line stars provide us with a list of HAeBe candidates to which we apply additional constraints, like NIR (§3.2) and IRAS fluxes (§4.1) to select stars with inner dusty disks .

We use B-V colors from the Hipparcos Catalog In order to estimate the visual extinction A_V. Only the star HIP17561 in Perseus OB1 association does not have photometric information, so we take the V and B-V values from the SIMBAD data-base. The intrinsic $(B-V)_0$ color is obtained interpolating our spectral type in the table of colors for main sequence stars given by Kenyon & Hartmann (1995, hereafter KH95). We use the extinction relation from Cardelli, Clayton, & Mathis (1989) and the value of total-to-selective extinction for normal interstellar reddening (R_V=3.1). Although in moderately and highly embedded HAeBe this value is larger than that for normal interstellar reddening (e.g. Hernández et al. 2004; Whittet et al. 2001; Waters & Waelkens 1998), we use R_V=3.1 for our stars because they have low visual extinction ($A_V <$ 1 mag); differences in R_V imply differences in A_V (column 5 of Table 2) smaller than the error (column 6 of Table 2) propagated from errors in the spectral type and the photometric data.

---

[2] IRAF is distributed by the National Optical Astronomy Observatories, which are operated by the Association of Universities for Research in Astronomy, Inc., under cooperative agreement with the National Science Foundation.

3.2. Near Infrared Color Color Diagram

The HAeBe show significant excesses in the JHK diagram relative to their photospheric colors (Hillenbrand et al. 1992; Lada & Adams 1992). These excesses are associated with disk emission (Natta et al. 2001; Maheswar, Manoj, & Bhatt 2002; Dullemond et al. 2001; Dullemond & Dominik 2004a; Muzerolle, et al 2004). However, there are early type stars with emission lines, the CBe, which also show near infrared excesses from gaseous free-free emission, although they are not of PMS nature; these stars are often confused with HAeBe. To determine the actual regions in the JHK color-color diagram occupied by the HAeBe and the CBe, we have compared dereddened colors of samples of both types. The HAeBe sample is taken from Hernández et al. (2004) and the sample of CBe from Yudin (2001). The HAeBe, the CBe and the objects in each association were corrected for reddening using the relations from Cardelli, Clayton, & Mathis (1989). The dereddened 2MASS colors were converted into the standard CIT systems using the transformations from Carpenter (2001). The intrinsic colors of dwarf and giant stars in Johnson-Glass system were taken from Bessell & Brett (1988). We complete the earlier main sequence stars with photometric data from Koornneef (1983) transformed to the Johnson-Glass system (Cox 2000). The Johnson-Glass system system was converted to the CIT system using the transformation given in Bessell & Brett (1988).

In Figure 2, we plot dereddened colors of the sample of HAeBe (Hernández et al. 2004) on the JHK color-color diagram in three spectral ranges, earlier than B5, later than F0, and between B5 and F0. We selected stars with reliable 2MASS data as determined from their photometric quality flag. We complete the NIR data using photometry from Eiroa et al. (2001) and by de Winter et al. (2001). All these objects were corrected by reddening using the A_V calculated by Hernández et al. (2004) and the mean value of R_V adequate for this sample (R_V=5.0). We also plot in Figure 2 the dereddened colors of a sample of CBe from Yudin (2001), distinguishing stars with spectral type B5 or later, and spectral type earlier than B5. To get a homogeneous CBe sample, we selected objects with 2MASS photometry and with HIPPARCOS spectral type taken from the Michigan Catalogs (Houk & Cowley 1975; Houk 1978, 1982; Houk & Smith-Moore 1988). We used the B-V color from the Hipparcos catalog and the normal interstellar reddening law to estimate the A_V for the CBe.

The CBe and the HAeBe occupy separate regions in the JHK color-color diagram, with the CBe located in a relative small region near the blue end of the main sequence. In contrast, most of the HAeBe are distributed below the Classical T Tauri star (CTTS) locus defined by Meyer, Calvet, & Hillenbrand (1997), in a more extended band more or less parallel to the reddening vector, but displaced to the right of the reddening line from a B0 star (Figure 2). This clear difference on the JHK color-color diagram was noted previously by Lada & Adams (1992) using samples of HAeBe and Be stars, but the objects were not corrected for reddening, so the region occupied by the HAeBe in that paper was more spread out extending even above the CTTS locus. In Figure 2, there are two stars listed as HAeBe that appear on the CBe region. One of them is MC 1 (HBC324) which has spectral type A7 and emission at the forbidden lines [O I] λ6300, [O I] λ6363, [S II] λ6717 and [S II] λ6731 additional to the emission at Hα. The other star, BD+651637 (HBC730), has spectral type B4 with emission at Hα and Hβ and Fe II. These objects could be stars with nearly pole-on disks, where the contribution of the vertical wall at the dust destruction radius is negligible (Dullemond et al. 2001); however, no IRAS sources are associated with them. Additional studies of these stars are required to clarify if the lack of NIR excess is produced by a special geometry of the disk or by its absence. The object located above of the CTTS locus is the star V633 Cas (HBC3); the strong IRAS color suggests that the position of this object on the JHK color-color diagram does not arise from an underestimate of the reddening correction. This star is associated with complex reflection nebulae and has a class I-like companion at 6” north that could be contributing to the observed NIR excesses (Fukagawa et al. 2002; Lagage et al. 1993). The early F star located to the left from the B0 reddening line is BO Cep (HBC735) which has a double peak profile at Hα line. The 2MASS colors of this object are flagged as a source contaminated by nearby star.

We have extracted from the JHK$_s$ colors for stars in our sample from the 2MASS All Sky Survey. In general, the positions of the Hipparcos stars and their respective 2MASS sources match within 0.5”; only for the star HIP80473 in US the difference is larger than 1”. The object HIP111104 has JHK$_S$ magnitudes contaminated by nearby stars. Figure 3 shows the JHK color-color diagrams of the associations US (a), Per OB2 (b), Lac OB1 (c), Ori OB1a (d) and Ori OB1bc (e), and for the probable members of the cluster Trumpler 37 (f) from Contreras et al. (2002), indicating the stars with Hα in emission. Stars located in the HAeBe region are labeled with their respective Hipparcos numbers. We will discuss individual associations in §4.

3.3. Distances

Astrometric distances for the associations were obtained using the Hipparcos parallaxes of the stars in each association. We applied a χ^2 test over the distribution of distance of the stars in each association, changing the theoretical distance until a minimal value of χ^2 was obtained by comparing with the observational distance in the sample; in this way, we obtain a first guess for the distance of each stellar group. We calculated the standard deviation (σ) using the individual distances of the stars and this first guess of the distance. To improve our determination, we rejected those values with differences larger than 3 σ. Then we ran the χ^2 test on the improved distribution of parallaxes to obtain the value of distance reported in column 6 of Table 1. With our estimate, we reject less than 10% stars from the original sample. The errors reported in Table 1 are the uncertainty in the mean σ ($\frac{\sigma}{\sqrt{N}}$), where N is the number of stars used to calculate the distances in each association. Except for Lac OB2, our determination is in agreement with the previous values of distance calculated using Hipparcos data (de Zeeuw et al. 1999; Brown et al. 1999b).

We also estimated photometric distances fitting each sample to the ZAMS defined by Cox (2000) on the B-V, M_V color magnitude diagram. We applied a χ^2 test comparing the dereddened values of B-V and M_V of the stars in each association with the respective values of the ZAMS (Cox 2000). In each case we changed the distance of the association, used to calculated M_V, until a minimum value of χ^2 is obtained. We used a similar rejection criterion to the one described in the preceding paragraph to improve the χ^2 test. In this case, we also rejected stars with B-V>0.0 to avoid stars that have not yet reached the ZAMS. These estimates are less reliable since the method is dependent on the evolutionary status, metallicity of the stellar groups, presence of multiple systems and photometric calibration (e.g. Vandenberg & Poll 1989; Pinsonneault et al. 1998; Robichon et al. 1999; Carretta et al. 1999). However, except for Ori OB1bc which has a large number of stars above the ZAMS because of its youth, the photometric and astrometric distances are in good agreement within the errors estimated for each stellar group.

3.4. Hertzsprung-Russell diagrams

We calculated the stellar luminosity using the Hipparcos V magnitude corrected for reddening with A_V given in the column 5 of Table 2 (§3.1), bolometric corrections from KH95, and astrometric distances calculated in §3.3. The effective temperature was determined using our spectral types and the calibration by KH95. With these values we plot the HRD for each stellar group in Figure 4. As reference we plot the ZAMS, the evolutionary tracks for 0.2, 0.6, 1.0, 1.5, 2.0, 3.0 and 4.0 $M_\odot$from Palla & Stahler (1993) and for 5, 9 and 15 $M_\odot$ from Bernasconi (1996). For each association, we plot the isochrones from Palla & Stahler (1993) corresponding to the age range reported in Table 1. We derive masses for the stars in each stellar group by double interpolation on the tracks using the values of $T_{\rm eff}$ and luminosities calculated previously. This information is shown in Table 2.

4. Census of Herbig Ae/Be in the associations

Table 3 lists the emission line stars identified from their spectra in each association. Columns 1, 2 and 3 show the Hipparcos name, other name and the association to which the stars belong. Columns 4 and 5 give the EW_λ of the Hα and Hβ lines, respectively (see §3.1). Column 6 gives the type of star (HAeBe or CBe) based on the location of the stars on the dereddened JHK color-

color diagram (Figure 2, see §3.2). The associated IRAS source, if it exists, is given in column 7. The β index calculated following the method described in §4.1 is show in the last column. This information is used to identify stars with inner disks in each stellar group.

4.1. Upper Scorpius

Upper Scorpius is the youngest of the three subgroups which form the Scorpius-Centaurus association, the OB association nearest to the sun. The other two subgroups, Upper Centaurus Lupus and Lower Centaurus Crux with ages of 13 and 10 Myr (Brown et al. 1999a) extend southward of our telescope pointing limit. The age of US is about 5 Myr (de Geus, de Zeeuw, & Lub 1989; Blaauw 1991; Preibisch & Zinnecker 1999; Brown et al. 1999a; Preibisch et al. 2002). The distance reported by de Zeeuw et al. (1999) using Hipparcos parallaxes is in good agreement with the astrometric and photometric distances derived in §3.3. Four objects exhibit emission in the Hα line. Two of these stars (HIP79476 and HIP81624) are located in the HAeBe region on the JHK color-color diagram, the other two (HIP78207 and HIP80569) are close to the CBe region (see Table 3 and Figure 3a).

The SEDs of the Hα emission stars confirm the classification in HAeBe or CBe based on the location in the JHK color-color diagram. Vieira et al. (2003) defined an spectral index (β) using the ratio of the IRAS flux at 12μm (F$_{12}$) to the flux in the visual band (F$_V$), to discriminate HAeBe from weaker infrared sources as CBe or Vega-like stars. Specifically, the index β is defined as

$$\beta = 0.75 \log{(F_{12}/F_V)} - 1 \tag{2}$$

HAeBe have spectral index $\beta \gtrsim -2.0$ (Vieira et al. 2003).

We calculated fluxes for each Hα emission star using the B, V, I$_c$ (Esa 1997) and J, H, K$_S$ (Cutri et al 2003) magnitudes corrected by reddening and the flux density for Vega (Cox 2000) at each band. Figure 5 shows the SEDs of the emission line star in US. Stars labeled as HAeBe from the JHK color-color diagram, have $\beta > -2$, characteristic of star with disks (Vieira et al. 2003).

All the stars in the sample, including the HAeBe, are located near or on the main sequence in the HRD (Figure 4a), indicating that the members of this sample have common properties. Only the star HIP80569, labeled as a CBe, has a slightly different position in this diagram, and its membership may have to be reviewed. Most of the lower mass stars in the sample follow the isochrones between 4 and 6 Myr, in agreement with the age reported for the association.

We identify the Herbig Ae/Be stars with stars with inner optically thick disks (§1), and use their numbers relative to the total to find the inner disk frequency (%F$_{disk}$) in each association. To analyze the fraction of stars with inner disks, we limited the sample to the spectral type range B5-F0. The presence of disks around stars earlier than B5 is not well established, possibly due to the rapid evolution of these objects which disperse the surrounding dust and gas in about 1 Myr (Fuente et al. 2002; Natta et al. 2000). Among the 93 objects observed in US, 13 have spectral types earlier than B5, 20 have spectral types later than F0, and 60 have spectral types between B5 and F0 (N_{B5-F0}); of these, only two objects can be labeled as stars with inner disks (N_{disk}). This indicates that in US 3.3 ± 1.3% of the intermediate mass stars have inner disks. The error is calculated from the ratio $\%F_{disk}/\sqrt{N_{disk}}$.

We explored the NIR properties of the 11 stars classified as early members (5 stars have spectral type between B5 and F0) by de Zeeuw et al. (1999) for which we did not obtain spectra. On the JHK color-color diagram, these stars fall to the left of the reddening vector from the B0 star, near the dwarf standard sequence. Since these data are not corrected by reddening, they must have small values of A_V and no NIR excess. Thus, these stars are unlikely to have inner disks. With these stars, $\%F_{disk} = 3.1$, which is within the errors of our original estimate.

4.2. Perseus OB2

Using photometric studies, Gimenez & Clausen (1994) found an age 10-15 Myr for Per OB2; Brown et al. (1999a) give an age between 4 and 8 Myr citing ages reported by different authors (see also, de Zeeuw et al. 1999). However, the ages reported for the open cluster IC348, a concentration of stars embedded in Per OB2, are in general younger: 5-20 Myr (Strom, Strom, & Carrasco 1974), 5-7 Myr (Lada & Lada 1995), 3-7 Myr (Trullols & Jordi 1997), and 1.3 - 3.0 Myr (Herbig 1998). Some authors suggest that the Per OB2 association consists of two subgroups (Herbig 1998; Hakobyan et al 2000; Belikov et al. 2002a,b). In particular, Herbig (1998) uses spectroscopic considerations based on the presence of Hα to suggest that IC 348 is projected upon an older population of stars. This conclusion was supported by Belikov et al. (2002a) using astrometric data. Since most of the stars in our sample are located outside of IC348, we adopt the age given by Brown et al. (1999a), which is older that the age estimated by Herbig (1998) for IC348. The distance reported by de Zeeuw et al. (1999) is in good agreement with the astrometric and photometric distances derived in §3.3.

In our sample of 40 stars, which include all the early members listed by de Zeeuw et al. (1999), we do not find stars with emission lines or NIR excess (see Figure 3b). Thus, the inner disk frequency in this stellar group is 0±4.3, where the error was calculated assuming one HAeBe in our sample. However, the lack of stars with inner disks in Per OB2 could be due to the low number of objects in the sample (N_{B5-F0}=23).

Figure 4b shows the HRD for Per OB2. The five stars later than G0 are unlikely to be members of Per OB2. We also show the isochrones for 4 and 8 Myr, but the lack of low mass stars prevents us from making a firm statement regarding the age of the association.

4.3. Lacerta OB1

Lacerta OB1 is a moderately sparse group. Using proper motions and radial velocities, Blaauw (1958) divided the region into two subgroups, an older and more sparse group extended to the northeast and named 1a, and other more concentrated group in the vicinity of the star HIP111841 (10 Lac). The photometric ages derived for 1a and 1b are 16 and 12 Myr, respectively (Blaauw 1964; Brown et al. 1999a). Using Hipparcos parallaxes, de Zeeuw et al. (1999) calculated a distance which is significantly smaller than previous estimates (Blaauw 1964; Lesh 1969; Crawford & Warren 1976). The astrometric distance calculated in §3.3 for this association is about 3σ larger than the value given by de Zeeuw et al. (1999), and in better agreement with our photometric estimate and the values given by others authors.

Out of the 82 stars observed in this work, 27 have spectral types earlier than B5, 3 have spectral types later than F0 and 52 have spectral types between B5 and F0; only four of these objects exhibit emission at Hα. All these objects are located in the CBe region on the JHK color-color diagram (Figure 3c), so we conclude that do not detect any star with an inner disk.

The Hα emission objects do not have associated IRAS sources. However, as the IRAS survey is complete to about 0.4, 0.5, 0.6, and 1.0 Jy at 12, 25, 60, and 100 μm (Joint IRAS Science Working Group 1988), we can calculate an upper limit for the β index; for the emission line objects the index is always less than -2.0, confirming the results derived from NIR colors. In Figure 6, we plot the SEDs for HIP110476, HIP112148, HIP111546 and HIP113226 with the upper limit of the IRAS fluxes. We then derive an inner disk frequency of 0 ± 1.9 % in Lac OB1. The statistical error was calculated assuming the presence of one HAeBe star.

Only one star listed by de Zeeuw et al. (1999) as an early type member was not observed in this work (HIP111841). However, the colors of HIP111841, not corrected for reddening, fall near the standard main sequence in the JHK diagram. This indicates that this star does not have NIR colors characteristic of HAeBe and does not change the results obtained previously.

4.4. Orion OB1a

Orion OB1a is the older group of the Orion OB1 association (see §2.2), one of the largest and nearest regions with active star formation. The age reported for this group ranges from 4 Myr (Lesh 1968) to 12 Myr (Blaauw 1991; Brown, de Geus, & de Zeeuw 1994). Using photometric variability and spectroscopic confirmation to select low mass members belonging to OB1a, Briceño et al. (2004) calculated an age of 7-10 Myr for this stellar group. We adopt this age for Ori OB1a. The distance reported by Brown et al. (1999b) using the average parallax of 61 Hipparcos stars is in good agreement with our estimates (see §3.3).

In our sample of 114 stars, we have 80 stars with spectral types in the range B5 and F0, 25 stars with spectral types earlier than B5 and 9 objects with spectral types later than F0. Six stars in our sample show emission at Hα line (HIP25258, HIP25299, HIP25302, HIP25655, HIP26476 and HIP26481). In addition, in the star HIP25299 we find that Hα is in absorption but filled in when compared to an A8 standard. An Hα emission line with relative small EW$_\lambda$ is visible in the higher resolution spectra of this star obtained by the EXPORT consortium (Merin 2004). In addition, the EXPORT multi-epoch spectra show variability in this line. So, we have included HIP25299 as an emission line star. The emission line stars show similar locations on the HRD (Figure 4d) as other members of the association.

Figure 3d shows that HIP25299 and HIP25258 are located in the HAeBe region on the JHK color-color diagram, while the other four emission line stars are likely to be CBe. In Figure 7 we plot the SEDs for the emission line stars. The β index calculated for these stars confirms the results obtained previously; namely, stars located in the CBe region (HIP25302, HIP25655, HIP26476 and HIP26481) on the JHK color-color diagram have β characteristic of stars without inner disks (< -2.0), while the β index of HIP25299 and HIP25258 confirms the presence of inner disks. From this analysis we obtain an inner disk frequency of 2.5 ± 1.8 % for Ori OB1a.

4.5. Orion OB1bc

As discussed in §2.2, we have combined the associations Ori OB1b and Ori OB1c as defined by Warren & Hesser (1977a) into one. These authors reported ages of 5.1 Myr and 3.7 Myr for Ori OB1b and Ori OB1c, respectively. Later, Blaauw (1991) estimated ages of 7 Myr for Ori OB1b and 3 Myr for Ori OB1c. In contrast, , Brown, de Geus, & de Zeeuw (1994) suggest that Ori OB1b is younger than Ori OB1c, deriving ages of 1.7±1.1 and 4.6±2.0, respectively. However, OB1c is more spatially related to the youngest sub-association Orion OB1d (1Myr; Hillenbrand 1997) and contains large quantities of dust and gas (see Figure 1). Therefore, Ori OB1c could be co-eval or younger than Ori OB1b, which has an age of 3-5 Myr (Briceño et al. 2004). In any event, in this contribution we assume a range of age that includes most of the age estimates for both Ori OB1b and Ori OB1c, 3.5±3 Myr. Using Hipparcos data, Brown et al. (1999b) found that Ori OB1b and Ori OB1c are located at similar distances, 440 pc for 1b and 460 pc for 1c. These values are in good agreement with our astrometric distance calculated for the combined group Ori OB1bc (§3.3).

In our sample of 110 stars, we have 77 stars with spectral types in the range B5 and F0, 26 stars with types earlier than B5, and 7 objects with types later than F0. We detect six stars with Hα in emission. Figure 3e shows the position of the emission line stars on JHK color-color diagram. Objects HIP27452 and HIP27842 clearly appear in the CBe region on this diagram, while stars HIP25258, HIP25299 and HIP25302 have NIR excesses characteristic of HAeBe. HIP26500 is located between the CBe region and the HAeBe region. This star is a double system composed by stars with similar spectral types (Guetter 1976). An IRAS source is located 13" form HIP26500, and there are other possible objects associated with this IRAS source. We derived the SED and β index assuming that this IRAS source is associated with HIP26500 (β=-2.2) and using the completeness limit of the IRAS catalog (β <-2.5). However, the IRAS fluxes do not help to determine if this star is a CBe or a HAeBe star, because the β index is close to the limit defined by Vieira et al. (2003). For the other stars located in the CBe star region on the JHK color-color diagram, HIP27452 and HIP27842, the index β confirms the absence of disks. The remaining Hα emission stars, HIP26752, HIP27059 and HIP26955, show clear evidence of being HAeBe. Figure 8 shows the SED for the emission line stars in Ori OB1bc. Using the bona fide HAeBe, the fraction of inner disks present in Ori OB1bc is 3.8 ± 2.2 %. If we include the object HIP26500 as HAeBe, the fraction increases to 5.1 ± 2.6 %.

A small number of stars located around l=206° and b=-24° are not spatially related to dust or gas (Figure 1). It is possible that this group has different age and distance than those of Ori OB1bc; however, since there few of these stars, they are not likely to affect the inner disk frequency determination.

Figure 4e shows that most of the stars are located between the isochrones corresponding to the age range estimated for this stellar group (3.5 ± 3 Myr); the emission line stars show similar locations on the HRD as other members of the association.

4.6. Trumpler 37

We studied the inner disk frequency in Trumpler 37 (Tr 37) using the spectral types, extinctions and membership defined by Contreras et al. (2002). Tr 37 lies in the Cep OB2 association at a distance of 900 and with an age of 3-5 Myr. The spectroscopy was done using the same instrumental setup as for the other stellar groups studied in this contribution (see §2.2).

Out of 66 stars defined by Contreras et al. (2002) as probable members, 56 have spectral types between B5 and F0. Only 3 of these stars exhibit emission at Hα, MVA 437, MVA 426 and KUN 314S. The star KUN 341S is presumably heavily veiled by accretion onto the central star , and no spectral type could be assigned (Contreras et al. 2002). The other two stars were classified as B7.

We used 2MASS data to infer the presence of inner disks in the Hα emission objects. We corrected for reddening the JHK$_S$ magnitudes using the values of A$_V$ calculated by Contreras et al. (2002). The star MVA 437 falls in the CBe region while the star MVA 426 is located in the HAeBe region on the JHK color-color diagram (Figure 3f). The star KUN 314S does not have a determination of A$_V$ in Contreras et al. (2002) due to its high veiling. However, we can use the average extinction A$_V$=1.67±0.42 for Trumpler 37 calculated by Sicilia-Aguilar et al. (2004a) from a sample of low mass stars in the cluster to correct for reddening the J-H and H-K$_S$ colors. To support the use of the mean extinction for this star, we used this value of A$_V$ to correct the near infrared colors of the northern companion of the system, KUN 314N, and found the colors to correspond to those of an early G type star on the standard main sequence. This type is consistent with the spectral type G2 that we obtained from analysis of an unpublished spectrum of this star, which does not exhibit any emission features. With this reddening correction, the colors of KUN 314S are located between the CBe region and the HAeBe region, so we do not have clear evidence for an inner disk around this star. Also, this star does not have an associated IRAS source so we can only estimate an upper limit for β (see Table 3 and Figure 9). If we assume this object to be a HAeBe star, the resulting inner disk frequency for intermediate mass stars in Tr 37 is $4.3 \pm 3.0\%$. Otherwise we obtain a value of $2.2 \pm 2.2\%$

5. The inner disk frequency in intermediate mass stars

In sections 4.1 to 4.6 we determined the relative numbers of Herbig Ae/Be stars in each OB association, and identifying these stars with stars with inner disks, we estimated the inner disk frequency in intermediate mass stars. In Figure 10, we plot this frequency as a function of the age of the stellar group.

We compare our determinations of inner disk frequencies with similar quantities in low mass stars. In Figure 10 we show estimates for NGC2024, the Trapezium, IC348, NGC2264 and NGC2362 from Haisch, Lada, & Lada (2001), for Taurus (KH95), for Chameleon I (Gómez & Kenyon 2001), and for NGC7129 (Gutermuth et al. 2004).

We also include in Figure 10 the disk frequencies in low mass stars in Ori OB1a and 1b, which we calculate from the number of stars in Briceño et al. (2004) which show excesses relative to the main sequence in the JHK diagram. We assume that a star has an excess if $(\mathrm{H-K})_0 - (\mathrm{H-K})_{\mathrm{KH}} > 2\sigma_{\mathrm{KH}}$, where $(\mathrm{H-K})_0$ is the dereddened color, $(\mathrm{H-K})_{\mathrm{KH}}$ is the intrinsic color for the spectral type of the star taken from KH95, and $\sigma_{\mathrm{KH}} = 0.04$, which is the typical dispersion for Weak T Tauri stars (or disk-less stars, Kenyon & Hartmann 1995). Using this criterion, we find a disk frequency of $7.4 \pm 3.4\%$ for Ori OB1a and $17.4 \pm 3.6\%$ for Ori OB1b.

Parenthetically, we note that the frequencies determined from near infrared excesses in Ori OB1 are lower than the frequencies estimated from the relative numbers of CTTS in these associations, $10 \pm 4\%$ for Ori OB1a and $23 \pm 4\%$, by Briceño et al. (2004). These latter fractions refer to disks which are still accreting mass onto the star, as indicated by the presence of strong Hα emission characteristic of the CTTS (Muzerolle, Calvet, & Hartmann 2001). The lower fraction of inner dusty disks compared to accreting disks is consistent with our findings in (Calvet et al. 2004b), where we show evidence for significant dust evolution in the disks of Ori OB1, and suggests that regions like Ori OB1 harbor a number of transition objects like TW Hya (Calvet & D'Alessio 2001; Uchida et al 2004), with significant clearing of small dust particles in their inner disks.

The inner disk frequency in the Herbig Ae/Be stars is much lower than in the low mass stars in the age range 3 - 15 Myr. In addition, we do not see any indication of the strong decrease in disk frequency at ages 3-5 Myr in the low mass stars; rather, the inner disk fraction in HAeBe starts out already very low at 3 Myr ($\sim 2-5\%$) and then slowly decreases with time up to ~ 15 Myr when it has fallen to essentially zero. The lifetimes of disks seem to depend on the stellar mass, as suggested by Haisch, Lada, & Lada (2001); for intermediate mass stars, the inner disks dissipate more quickly than for the low mass stars.

Several possibilities may explain the mass dependence of the disks lifetimes. Calvet et al. (2004a) extended the correlation between mass accretion rate ($\dot{\mathrm{M}}$) and stellar mass (M_*) from Muzerolle et al. (2003a) to the intermediate mass stars, up to $\sim 3.5\mathrm{M}_\odot$; in particular, they found that $\dot{\mathrm{M}} \propto M_*^2$. On the other hand, the ratio of disk mass (M_D) to M_* is found to be approximately constant for stars with spectral type A0-M7 (Natta et al. 2000; Fuente et al. 2003). If the lifetimes of disks are determined by viscous evolution, which controls the accretion rate onto the star, the time for the disk to disappear by accretion processes can be estimated as the ratio $\mathrm{M}_D/\dot{\mathrm{M}}$, so the viscous lifetime of the disk is $\propto M_*^{-1}$.

Grain growth and settling toward the midplane in the disk can decrease the height of the inner wall of the disk and so decrease the NIR contribution from the inner disk (Calvet et al. 2004a). Following Dullemond & Dominik (2004b), in absence of turbulent stirring, the settling speed is given by

$$V_{sett} \propto \frac{M_* \, z \, m}{r^3 \, \rho(z)} \tag{3}$$

where z and r give the vertical and radial location of a particle with mass m that is settling, and $\rho(z)$ is the gas density in the disk, which decreases exponentially with z away from the midplane. V_{sett} is proportional to the mass of the star, so settling is expected to be more effective in the inner disks of HAeBe than in their low mass counterparts. Thus, the processes which lead to the dissipation of inner disk, that is, viscous and dust evolution are expected to occur in shorter time-scales in more massive stars.

6. Summary and Conclusions

In this contribution we studied the presence of inner disks around intermediate mass pre-main sequence stars in 5 stellar groups with range of ages from 3 to 16 Myr. The stars were selected from the Hipparcos catalog. The astrometric membership for US, Per OB2 and Lac OB1 associations was determined from de Zeeuw et al. (1999). The stars in Orion OB1 were selected as members using astrometric and photometric constrains (Brown, de Geus, & de Zeeuw 1994; Brown et al. 1999b) and divided in two groups, Ori OB1a and Ori OB1bc, with different ages and distances. We obtained spectra for 440 stars in these OB associations, from which we have determined spectral types, visual extinctions, $\mathrm{T_{eff}}$, luminosities and the presence of emission at Hα. We also included data for the cluster Trumpler 37 in the association Cep OB2, with data from Contreras et al. (2002).

We compared the dereddened J-H and H-K colors of a samples of HAeBe stars (Hernández et al. 2004) and CBe (Yudin 2001) in order to estimate the loci of these objects, showing that the HAeBe and the CBe occupy well defined different regions on this diagram.

We identified the Herbig Ae/Be stars in each association using the following criteria (1) Hα emission, (2) location in the HAeBe region of the JHK diagram, (3) strong IRAS fluxes with (β index > -2; Vieira et al. 2003). We identified 2 HAeBe in Upper Scorpius, 0 HAeBe in Perseus

OB2, 0 HAeBe in Lacerta OB1, 2 HAeBe in Orion OB1a, 4 HAeBe in Orion OB1bc and 2 HAeBe in Trumpler 37. From these identifications, we estimate a disk frequency of 3.3±1.7%, 0±4.4%, 0±1.9%, 2.5±1.7%, 5.1±2.0%, 4.3±1.8%, respectively. We have compared the inner disk frequency in intermediate mass stars (HAeBe star) with that for low mass stars in a number of stellar groups taken from the literature, and estimated by us for Ori OB1 from the sample of Briceño et al. (2004). We find that stars with inner disks are more frequent in low mass stars than in intermediate mass stars. Particularly, for the youngest associations (Ori OB1bc and Tr 37) the inner disk frequency for intermediate mass stars is $\sim$ ten times lower than the inner disk frequency reported for low mass stars. Although the inner disk frequency in intermediate mass stars tends to decrease slowly with age, we find no evidence of the strong decrease in the inner disk frequency observed in low mass stars at 3-5 Myr. Studies of intermediate mass stars in stellar groups younger than 3 Myr are required to determine in which age range, if any, a similar strong decrease with age occurs. We suggest that the lower inner disk frequency in intermediate mass stars is a result of more rapid mechanisms of inner disk dispersal (accretion, dust growth and settling toward the midplane).

This contribution suggests that most of the stars in the range of mass of the HAeBe disperse their inner disks in a timescale shorter than 3 Myr; in contrast, the inner disk frequency of low mass stars in this age range is larger than 50%. Samples of younger stellar groups are required to determined when the most of the intermediate mass stars disperse their inner disks.

7. Acknowledgments

We thank Francesco Palla to provide us the isochrones and evolutionary tracks of PMS stars, Bruno Merin for sending us the multi-epoch spectra of the star HIP26955, Thomas Megeath for comments about the association NGC 7129, Robert Wilson for providing with the ^{13} CO map of the Orion region, and Charlie Lada for useful comments. We also thank Susan Tokarz of the SAO Telescope Data Center for carrying out the data reduction, and Michael Calkins for obtaining some of the spectra. This publication makes use of data products from the Two Micron All Sky Survey, which is a joint project of the University of Massachusetts and the Infrared Processing and Analysis Center/California Institute of Technology, funded by the National Aeronautics and Space Administration and the National Science Foundation. This work was supported in part by NASA grants NAG5-9670 and NAG10545, NSF grant AST-9987367 and grant No. S1-2001001144 of FONACIT, Venezuela.

REFERENCES

van den Ancker, M. E., Thé, P. S., Feinstein, A., Vazquez, R. A., de Winter, D., & Perez, M. R. 1997, A&AS, 123, 63

Bally, J., Stark, A. A., Wilson, R. W., & Langer, W. D. 1987, ApJ, 312, L45

Belikov, A. N., Kharchenko, N. V., Piskunov, A. E., Schilbach, E., Scholz, R.-D., & Yatsenko, A. I. 2002a, A&A, 384, 145

Belikov, A. N., Kharchenko, N. V., Piskunov, A. E., Schilbach, E., & Scholz, R.-D. 2002b, A&A, 387, 117

Bernasconi, P. A. 1996, A&AS, 120, 57

Bessell, M. S. & Brett, J. M. 1988, PASP, 100, 1134

Blaauw, A. 1952, Bull. Astron. Inst. Netherlands, 11, 405

Blaauw, A. 1958, AJ, 63, 187

Blaauw, A. 1964, ARA&A, 2, 213

Blaauw, A. 1991, NATO ASIC Proc. 342: The Physics of Star Formation and Early Stellar Evolution, 125

Blake, G. A. & Boogert, A. C. A. 2004, ApJ, 606, L73

van Boekel, R., Waters, L. B. F. M., Dominik, C., Bouwman, J., de Koter, A., Dullemond, C. P., & Paresce, F. 2003, A&A, 400, L21

Cesar Briceno, Nuria Calvet, J. Hernández, A.K. Vivas, Lee Hartmann, J.J. Downes and Perry Berlind, 2004, submitted to AJ.

Brown, A. 1950, ApJ, 112, 225

Brown, A. G. A., de Geus, E. J., & de Zeeuw, P. T. 1994, A&A, 289, 101

Brown, A. G. A., Blaauw, A., Hoogerwerf, R., de Bruijne, J. H. J., & de Zeeuw, P. T. 1999a, NATO ASIC Proc. 540: The Origin of Stars and Planetary Systems, 411

Brown, A. G., Walter, F. M., & Blaauw, A. 1999b, in ASP Conf. Ser., The Orion Complex Revisited, ed. M.J. McCaughrean & A. Burkert.

Brown, A. G. A. 2001, Revista Mexicana de Astronomia y Astrofisica Conference Series, 11, 89

de Bruijne, J. H. J. 1999, MNRAS, 306, 381

Calvet, N. & D'Alessio, P. 2001, ASP Conf. Ser. 235: Science with the Atacama Large Millimeter Array, 205

Calvet, N., Muzerolle, J., Briceño, C., Hernández, J., Hartmann, L., Saucedo, J. L., & Gordon, K. D. 2004a, AJ, 128, 1294

Calvet N., Briceño, Hernández J., Hoyer S., Hartmann L., Sicilia-Aguilar A., Megeath S., and D'Alessio P., 2004b, AJ (in press)

Cardelli, J. A., Clayton, G. C., & Mathis, J. S. 1989, ApJ, 345, 245

Carpenter, J. M. 2001, AJ, 121, 2851

Carretta, E., Gratton, R. G., Clementini, G., & Fusi Pecci, F. 1999, ASP Conf. Ser. 167: Harmonizing Cosmic Distance Scales in a Post-HIPPARCOS Era, 255

Chini, R., Hoffmeister, V., Kimeswenger, S., Nielbock, M., Nürnberger, D., Schmidtobreick, L., & Sterzik, M. 2004, Nature, 429, 155

Contreras, M. E., Sicilia-Aguilar, A., Muzerolle, J., Calvet, N., Berlind, P., & Hartmann, L. 2002, AJ, 124, 1585

Cox, A. N. 2000, Allen's astrophysical quantities, 4th ed. Publisher: New York: AIP Press; Springer, 2000. Edited by Arthur N. Cox. ISBN: 0387987460,

Cutri R.M., Skrutskie M.F., Van Dyk S., Beichman C.A., Carpenter J.M., Chester T., Cambresy L., Evans T., Fowler J., Gizis J., Howard E., Huchra J., Jarrett T., Kopan E.L., Kirkpatrick J.D., Light R.M, Marsh K.A., McCallon H., Schneider S., Stiening R., Sykes M., Weinberg M., Wheaton W.A., Wheelock S., Zacarias N. 2003, 2MASS All-Sky Catalog of Point Sources, University of Massachusetts and Infrared Processing and Analysis Center.

Crawford, D. L. & Warren, W. H. 1976, PASP, 88, 930

Davies, J. K., Evans, A., Bode, M. F., & Whittet, D. C. B. 1990, MNRAS, 247, 517

Dullemond, C. P., Dominik, C., & Natta, A. 2001, ApJ, 560, 957

Dullemond, C. P. & Dominik, C. 2004a, A&A, 417, 159

Dullemond, C. P. & Dominik, C. 2004b, A&A, 421, 1075

Eiroa, C.; Garzn, F.; Alberdi, A.; de Winter, D.; Ferlet, R.; Grady, C. A.; Cameron, A.; Davies, J. K.; Deeg, H. J.; Harris, A. W.; Horne, K.; Mern, B.; Miranda, L. F.; Montesinos, B.; Mora, A.; Oudmaijer, R.; Palacios, J.; Penny, A.; Quirrenbach, A.; Rauer, H.; Schneider, J.; Solano, E.; Tsapras, Y.; Wesselius, P. R., 2001, A&A, 365, 110

ESA, 1. 1997, The Hipparcos and Tycho Catalogs, ESA SP-1200.

Fabricant, D., Cheimets, P., Caldwell, N., & Geary, J. 1998, PASP, 110, 79

Finkenzeller, U. & Mundt, R. 1984, A&AS, 55, 109

Fuente, A., Martın-Pintado, J., Bachiller, R., Rodrıguez-Franco, A., & Palla, F. 2002, A&A, 387, 977

Fuente, A., Rodríguez-Franco, A., Testi, L., Natta, A., Bachiller, R., & Neri, R. 2003, ApJ, 598, L39

Fukagawa, M., et al. 2002, PASJ, 54, 969

Genzel, R. & Stutzki, J. 1989, ARA&A, 27, 41

de Geus, E. J., de Zeeuw, P. T., & Lub, J. 1989, A&A, 216, 44 .

Gimenez, A. & Clausen, J. V. 1994, A&A, 291, 795

Gómez, M. & Kenyon, S. J. 2001, AJ, 121, 974

Guetter, H. H. 1976, AJ, 81, 537

Gutermuth, R. A., Megeath, S. T., Muzerolle, J., Allen, L. E., Pipher, J. L., Myers, P. C., & Fazio, G. G. 2004, ArXiv Astrophysics e-prints, astro-ph/0406091

Haisch, K. E., Lada, E. A., & Lada, C. J. 2001, ApJ, 553, L153

Hakobyan, A. A., Hambaryan, V. V., Poghosyan, A. V., & Salukvadze, G. N. 2000, IAU Symposium, 200, 124P

Herbig, G. H. 1960, ApJS, 4, 337

Herbig, G. H. 1998, ApJ, 497, 736

Hernández, J., Calvet, N., Briceño, C., Hartmann, L., & Berlind, P. 2004, AJ, 127, 1682

Hillenbrand, L. A., Strom, S. E., Vrba, F. J., & Keene, J. 1992, ApJ, 397, 613

Hillenbrand, L. A. 1997, AJ, 113, 1733

Hoogerwerf, R. & Aguilar, L. A. 1999, MNRAS, 306, 394

Houk, N. & Smith-Moore, M. 1988, Michigan Spectral Survey, Ann Arbor, Dept. of Astronomy, Univ. Michigan (Vol. 4) (1988).

Houk, N. 1982, Michigan Spectral Survey, Ann Arbor, Dep. Astron., Univ. Michigan, 3 (1982).

Houk, N. & Cowley, A. P., 1975, VizieR Online Data Catalog III/31, Michigan catalog for the HD stars, vol. 1.

Houk, N., 1978, VizieR Online Data Catalog III/51, Michigan catalogs for the HD stars, vol. 2.

Joint IRAS Science Working Group 1988, IRAS Point Source Catalog (1988),

Kenyon, S. J. & Hartmann, L. 1995, ApJS, 101, 117

Koornneef, J. 1983, A&A, 128, 84

Lada, C. J. & Adams, F. C. 1992, ApJ, 393, 278

Lada, E. A. & Lada, C. J. 1995, AJ, 109, 1682

Lagage, P. O., Olofsson, G., Cabrit, S., Cesarsky, C. J., Nordh, L., & Rodriguez Espinosa, J. M. 1993, ApJ, 417, L79

Lagrange, A.-M., Backman, D. E., & Artymowicz, P. 2000, Protostars and Planets IV, 639

Lesh, R. J. 1968, ApJ, 152, 905

Lesh, R. J. 1969, AJ, 74, 891

Lorenzetti, D., Saraceno, P., & Strafella, F. 1983, ApJ, 264, 554

Maheswar, G., Manoj, P., & Bhatt, H. C. 2002, A&A, 387, 1003

Malfait, K., Bogaert E. & Walkens C. 1998, A&A, 331, 211

Mannings, V. & Sargent, A. I. 1997, ApJ, 490, 792

Mannings, V. & Sargent, A. I. 2000, ApJ, 529, 391

Merin, B. 2004, personal communication.

Meyer, M. R., Calvet, N., & Hillenbrand, L. A. 1997, AJ, 114, 288

Muzerolle, J., Hillenbrand, L., Calvet, N., Briceño, C., & Hartmann, L. 2003a, ApJ, 592, 266

Muzerolle, J., Calvet, N., Hartmann, L., & D'Alessio, P. 2003b, ApJ, 597, L149

Muzerolle, J., D'Alessio, P., Calvet, N., & Hartmann, L. 2004, ApJ (in press)

Natta, A., Grinin, V., & Mannings, V. 2000, Protostars and Planets IV, 559

Natta, A., Prusti, T., Neri, R., Wooden, D., Grinin, V. P., & Mannings, V. 2001, A&A, 371, 186

Palla, F. & Stahler, S. W. 1993, ApJ, 418, 414

Pinsonneault, M. H., Stauffer, J., Soderblom, D. R., King, J. R., & Hanson, R. B. 1998, ApJ, 504, 170

Preibisch, T. & Zinnecker, H. 1999, AJ, 117, 2381

Preibisch, T., Brown, A. G. A., Bridges, T., Guenther, E., & Zinnecker, H. 2002, AJ, 124, 404

Robichon, N., Arenou, F., Lebreton, Y., Turon, C., & Mermilliod, J. C. 1999, ASP Conf. Ser. 167: Harmonizing Cosmic Distance Scales in a Post-HIPPARCOS Era, 72

Schlegel, D. J., Finkbeiner, D. P., & Davis, M. 1998, ApJ, 500, 525

Sicilia-Aguilar, A., Hartmann, L. W., Briceño, C., Muzerolle, J., & Calvet, N. 2004a, AJ, 128, 805

Strom, S. E., Strom, K. A., & Carrasco, L. 1974, PASP, 86, 798

Trullols, E. & Jordi, C. 1997, A&A, 324, 549

Uchida, K. I.; Calvet, N.; Hartmann, L.; Kemper, F.; Forrest, W. J.; Watson, D. M.; D'Alessio, P.; Chen, C. H.; Furlan, E.; Sargent, B.; Brandl, B. R.; Herter, T. L.; Morris, P.; Myers, P. C.; Najita, J.; Sloan, G. C.; Barry, D. J.; Green, J.; Keller, L. D.; Hall, P., 2004, in preparation.

Vandenberg, D. A. & Poll, H. E. 1989, AJ, 98, 1451

Vieira, S. L. A., Corradi, W. J. B., Alencar, S. H. P., Mendes, L. T. S., Torres, C. A. O., Quast, G. R., Guimarães, M. M., & da Silva, L. 2003, AJ, 126, 2971

Warren, W. H. & Hesser, J. E. 1977a, ApJS, 34, 115

Warren, W. H. & Hesser, J. E. 1977b, ApJS, 34, 207

Waters, L. B. F. M. & Waelkens, C. 1998, ARA&A, 36, 233

Whittet, D. C. B., Gerakines, P. A., Hough, J. H., & Shenoy, S. S. 2001, ApJ, 547, 872

de Winter, D., van den Ancker, M. E., Maira, A., Thé, P. S., Djie, H. R. E. T. A., Redondo, I., Eiroa, C., & Molster, F. J. 2001, A&A, 380, 609

Yudin, R. V. 2001, A&A, 368, 912

de Zeeuw, P. T., Hoogerwerf, R., de Bruijne, J. H. J., Brown, A. G. A., & Blaauw, A. 1999, AJ, 117, 354

This preprint was prepared with the AAS LaTeX macros v5.2.

Table 1. Nearby Associations

Name	D_{Ref} pc	Age Myr	N	N_{spt}	D_{π} pc	D_{CMD} pc
Upper Scorpius	145 ± 2	5	120	93	144 ± 3	146 ± 5
Per OB2	318 ± 27	4−8	41	40	313 ± 13	300 ± 15
Lac OB1	368 ± 17	16	96	82	418 ± 15	438 ± 20
Ori OB1a	336 ± 16	7−10	124	114	335 ± 13	315 ± 8
Ori OB1bc*	438-462	1−7	121	111	443 ± 16	392 ± 20

Note. —

*The association Orion OB1bc have 2 sub-groups with similar distances and ages (Ori OB1b and Ori OB1c see §2.2)

Table 2. Stellar Properties

Hipparcos	Name	SpT	Error	A_V	$\sigma(A_V)$	J	J-H	$H-K_S$	$\log(T_{\rm eff})$	$\log(L/L_\odot)$	$M/M_\odot$
					Upper Scorpius						
HIP76071	HD138343	B9	1	0.28	0.14	7.11	0.03	0.08	4.02	1.64	2.5
HIP76310	HD138813	A1	2	0.09	0.23	7.16	-0.02	0.01	3.96	1.43	2.2
HIP78207[1]	HD142983	B1	2	0.62	0.41	5.10	0.27	0.24	4.44	3.66	12.8
HIP79439	HD145631	B9	1	0.63	0.15	7.05	0.00	0.11	4.02	1.65	2.5
					Perseus OB2						
HIP14145	BD+42 684	F8	1	0.23	0.13	8.60	0.21	0.06	3.79	1.19	2.1
HIP17172	HD22765	A5	2	0.31	0.24	8.83	0.01	0.10	3.91	1.37	2.0
HIP17313	HD22951	B1	1	0.65	0.18	5.00	-0.07	0.01	4.41	4.26	13.4

Note. — Table 2 is published in its entirety in the electronic edition of the *Astrophysical Journal*. A portion is shown here for guidance regarding its form and content.

[1] Stars with emission in Hα line (see table 3)

Table 3. Emission line stars

Hipparcos	Name	Assoc (Å)	EW$_\lambda$[Hα] (Å)	EW$_\lambda$[Hβ] loci	JHK	IRAS β	index Disk	Inner
HIP78207	48 Lib	US	-21.0	-0.1	Be	15553-1408	-3.2	N
HIP79476	V718 Sco	US	-0.6	···	HAeBe	16102-2221	-1.7	Y
HIP80569	HD148184	US	-36.4	-3.9	Be	16241-1820	-3.0	N
HIP81624	V2307 Oph	US	-11.9	···	HAeBe	16372-2347	-1.6	Y
HIP110476	BD+42 4370	Lac OB1	-18.7	-0.5	Be	···	<-2.4	N
HIP111546	HD214167	Lac OB1	-12.9	-0.1	Be	···	<-3.3	N
HIP112148	HD215227	Lac OB1	-23.1	-1.2	Be	···	<-2.7	N
HIP113226	HD216851	Lac OB1	-41.2	-2.4	Be	···	<-2.8	N
HIP25258	HD287823	Ori OB1a	-0.4	···	HAeBe	05215+0225	-2.0	Y
HIP25299	V346 Ori	Ori OB1a	-0.1	···	HAeBe	05221+0141	-2.0	Y
HIP25302	V1086 Ori	Ori OB1a	-3.8	···	Be	05221+0148	-3.1	N
HIP25655	V1372 Ori	Ori OB1a	-26.0	-1.4	Be	···	<-2.9	N
HIP26476	HD37330	Ori OB1a	-5.4	···	Be	···	<-2.8	N
HIP26481	HD37342	Ori OB1a	-5.6	···	Be	···	<-2.6	N
HIP26500 [2]	HD37371	Ori OB1bc	-4.3	···	···	···	<-2.5	?
HIP26752	HD37806	Ori OB1bc	-24.5	···	HAeBe	05385+0244	-2.0	Y
HIP26955	HD38120	Ori OB1bc	-21.6	-2.1	HAeBe	05407+0501	-3.1	Y
HIP27059	V351 Ori	Ori OB1bc	-0.9	···	HAeBe	05417+0007	-2.9	Y
HIP27452	HD38856	Ori OB1bc	-13.9	-0.6	Be	···	<-2.8	N
HIP27842	HD39557	Ori OB1bc	-24.0	-0.7	Be	···	<-2.7	N
···	MVA 426	Tr 37	-6.9	···	HAeBe	21365+5713	-2.0	Y
···	MVA 437	Tr 37	-8.3	···	Be	···	<-2.1	N
··· [2]	KUN 314S	Tr 37	-38.1	-3.9	···	···	<-1.8	?

The stars in Per OB2 do not show Hα in emission

[2] JHK loci between the HAeBe region and the CBe region

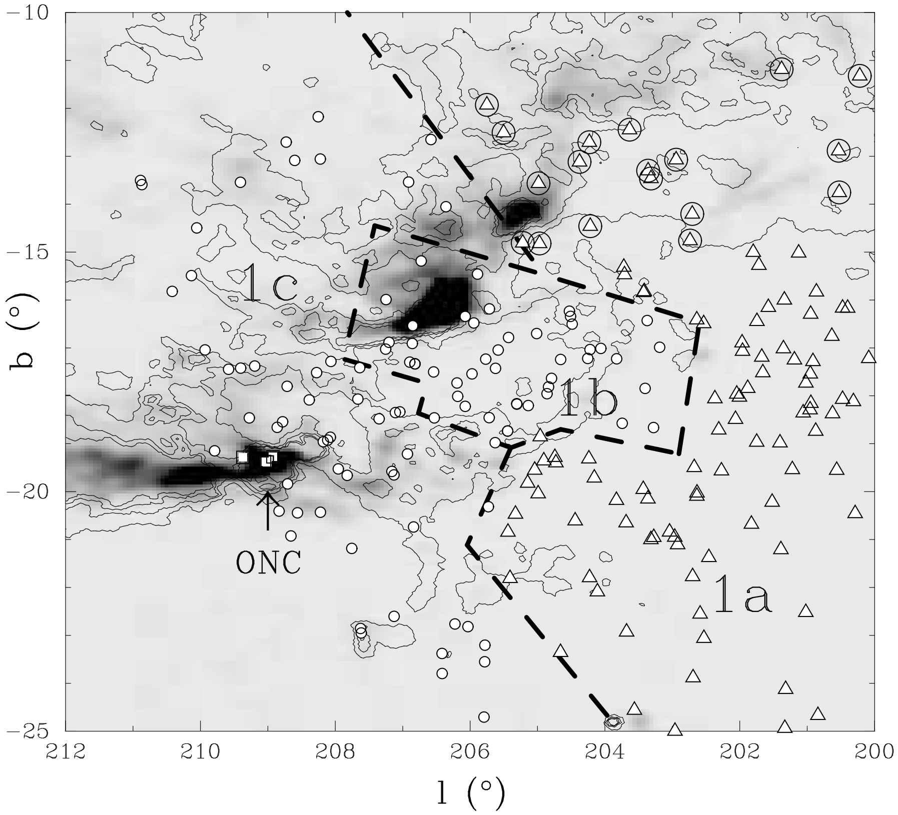

Fig. 1.— Spatial distribution of the Hipparcos stars in the Orion OB1 association. A map of ^{13}CO (Bally, Stark, Wilson, & Langer 1987) is shown in gray scale halftone, covering a range of integrated ^{13}CO emissivity from 0 to 35 K kms^1. The isocontours are estimators of galactic extinction (for A_V=1,2,3 and 4 mag) from the map of Dust Infrared Emission (Schlegel, Finkbeiner, & Davis 1998). The dashed lines are the limits of the sub-association from Warren & Hesser (1977a) for 1a (open triangles), 1b (open circles inside the dashed box) and 1c (open circles outside of the dashed box). A subset of stars in the region defined for Ori OB1a (Warren & Hesser 1977a) (open triangles surrounded by open circles), is spatially associated with molecular gas and dust; this subset is more likely related to the younger subassociation Ori OB1c.

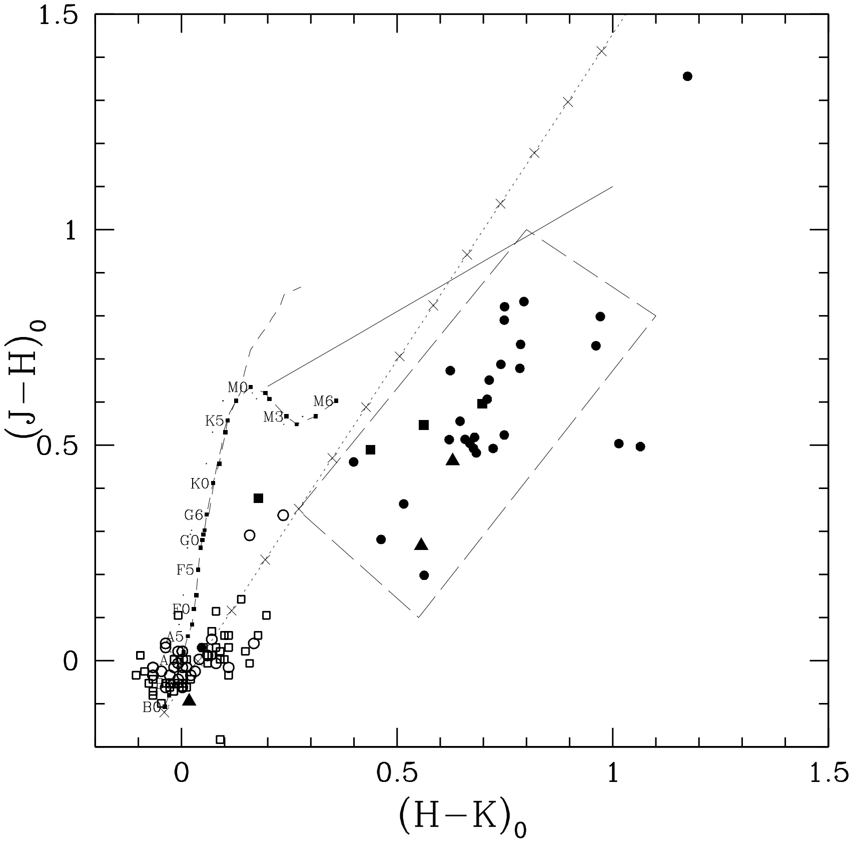

Fig. 2.— Loci of the HAeBe and the CBe on the JHK color-color diagram. The standard sequences from Bessell & Brett (1988) are shown in dashed lines. Colors of the HAeBe sample, taken from Hernández et al. (2004), corrected for reddening, fall to the right of the reddening line of a standard B0 star (dotted line). This line is calculated for R_V=3.1 with the reddening law of Cardelli, Clayton, & Mathis (1989); the tick-marks show intervals of A_V= 1. The reddening line for R_V=5.0 has similar slope (Cardelli, Clayton, & Mathis 1989), but larger spacing between tick-marks. The sample of HAeBe is separated in three spectral type ranges: earlier than B5 (solid filled triangles), between B5 and F0 (solid filled circles) and later than F0 (solid filled squares). The colors of the sample of CBe from Yudin (2001), corrected for reddening, concentrate in a region near of the blue end of the standard main sequence. The CBe are also separated in spectral type: B5 or later (open circles), earlier than B5 (open squares). As a reference, we plot the loci of CTTS (solid line) defined by Meyer, Calvet, & Hillenbrand (1997). It is apparent that the HAeBe and the CBe occupy different regions on the JHK diagram. The HAeBe are concentrated in a region (long dashed lines) on the JHK color-color diagram approximately defined by the vertices (J-H,H-K)=(0.27,0.35); (0.80,1.00); (1.10,0.80); (0.55 0.80). All the measurements were transformed to the CIT system (see §3.2)

.

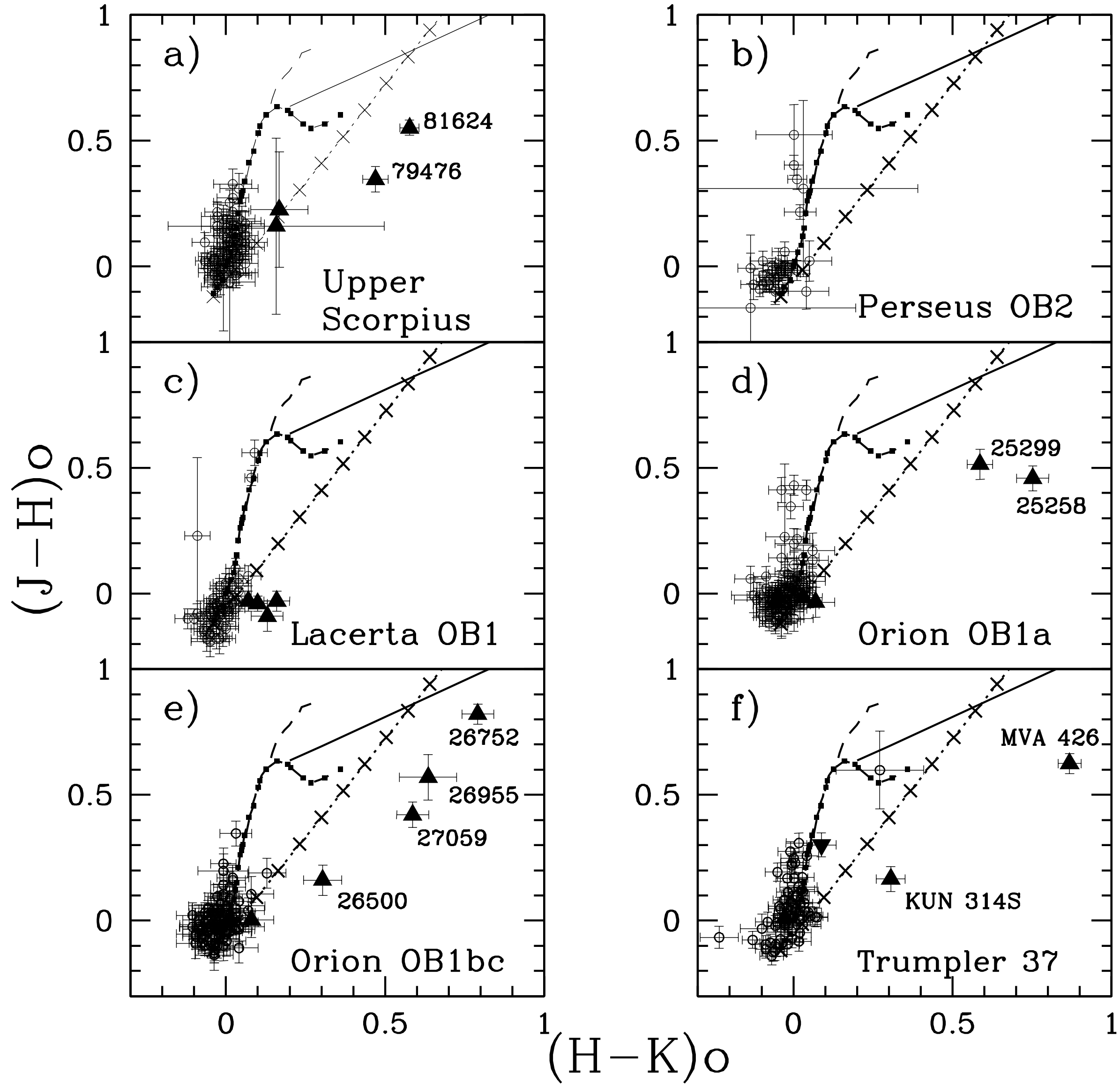

Fig. 3.— Dereddened J-H and H-K colors of the early type stars in the OB associations studied in this work (§4). Stars with emission in Hα are plotted as solid triangles. Stars without emission lines (open circles) concentrate on the main sequence or in the CBe region (see Figure 2). The inverse solid triangle in panel f is the star KUN314N (§4.6) Other symbols as in Fig. 2. Objects located in the HAeBe region are labeled with their number in the Hipparcos catalog. The error bars are estimated by propagating both the error in our spectral type determination and the error from the 2MASS catalog.

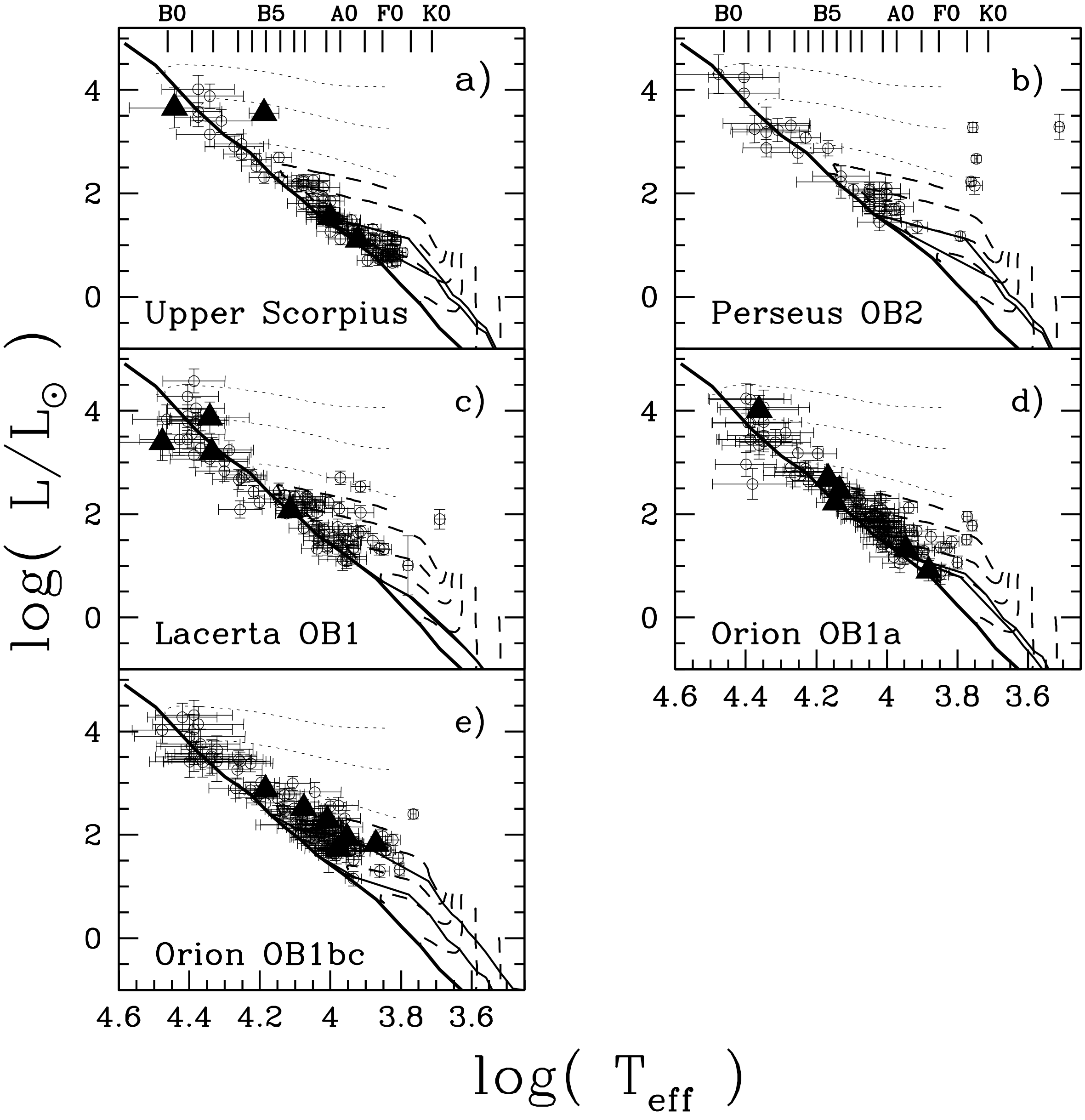

Fig. 4.— HR diagram for the Hipparcos stars in the OB associations studied in this work. Emission line stars are plotted as solid triangles while open circles indicate stars without emission. Isochrones from Palla & Stahler (1993) for the range of ages of each association in Table 1 (light solid lines) are shown, as well as evolutionary tracks from Palla & Stahler (1993) (dashed lines) corresponding to, from bottom to top, 0.2, 0.6, 1.0, 1.5, 2.0 3.0, and 4.0 M$_\odot$; tracks for 5, 9 and 15 M$_\odot$(dotted lines) are from Bernasconi (1996). The ZAMS is represented as a thick solid line. The emission line stars and the objects without emission share the same region in these plots.

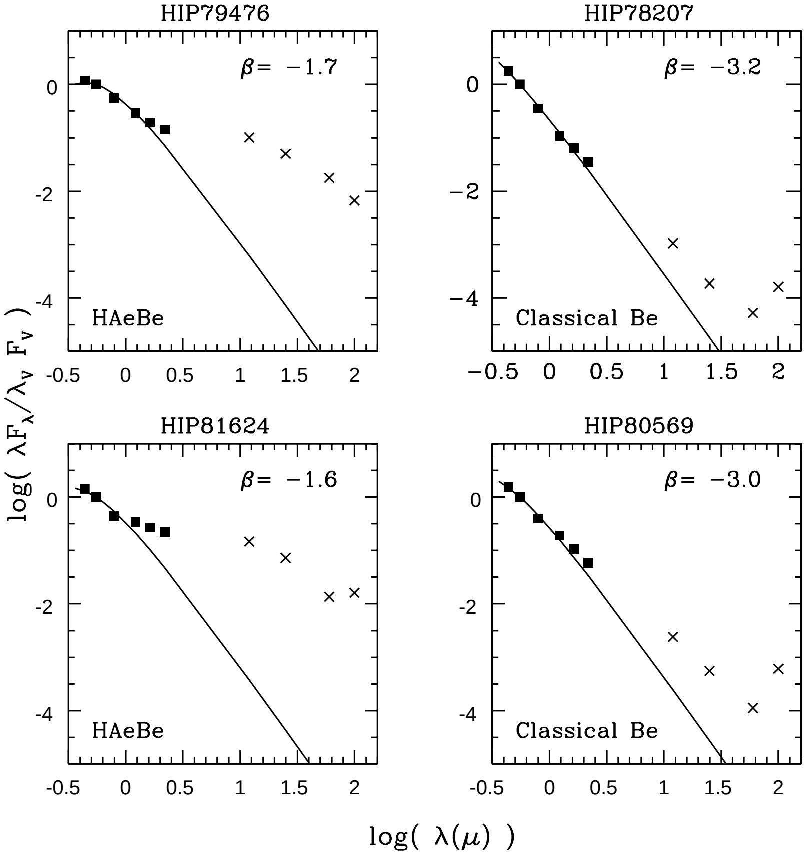

Fig. 5.— SEDs of the emission line stars in the Upper Scorpius OB association. Fluxes calculated from magnitudes in the B, V, I bands (Esa 1997) and the J, H, K bands (Cutri et al 2003), normalized to the flux at V, are plotted as solid squares. The IRAS fluxes at 12, 25 60 and 100 μm are represented by x's. We show that the β index defined by Vieira et al. (2003), §3.3, can separate the HAeBe (left column panels) from the CBe (right column panels)

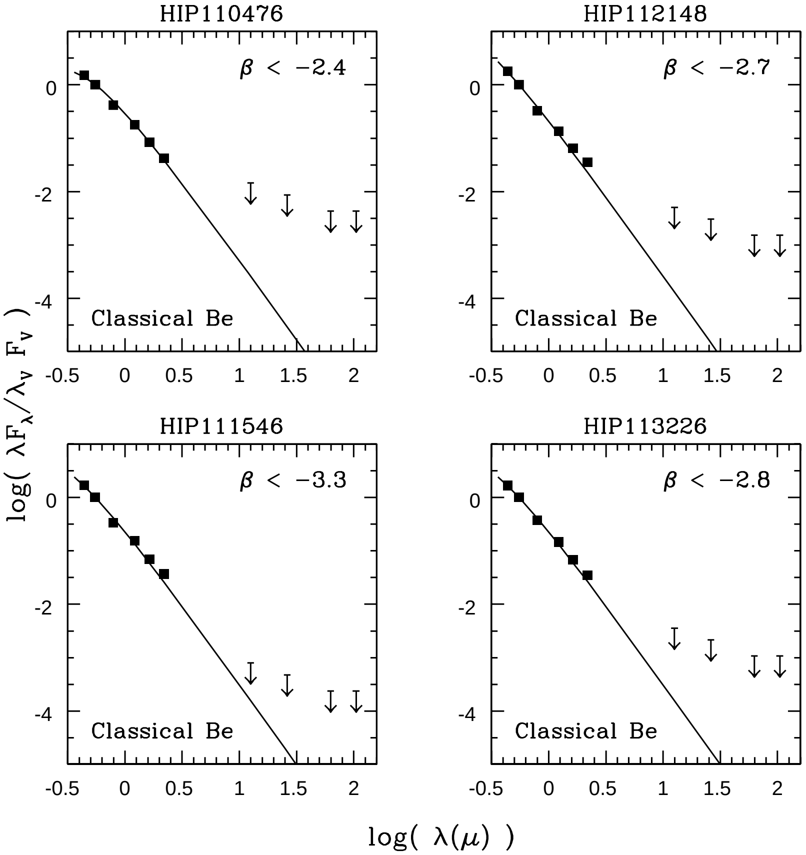

Fig. 6.— SEDs of emission line stars in Lac OB1. Labels as in Figure 5. The down arrows represent the completeness limit for the IRAS catalog for 12, 25, 60 and 100 μm (0.4, 0.5, 0.6 and 1.0 Jy, respectively). The presence of inner disks is unlikely in these stars.

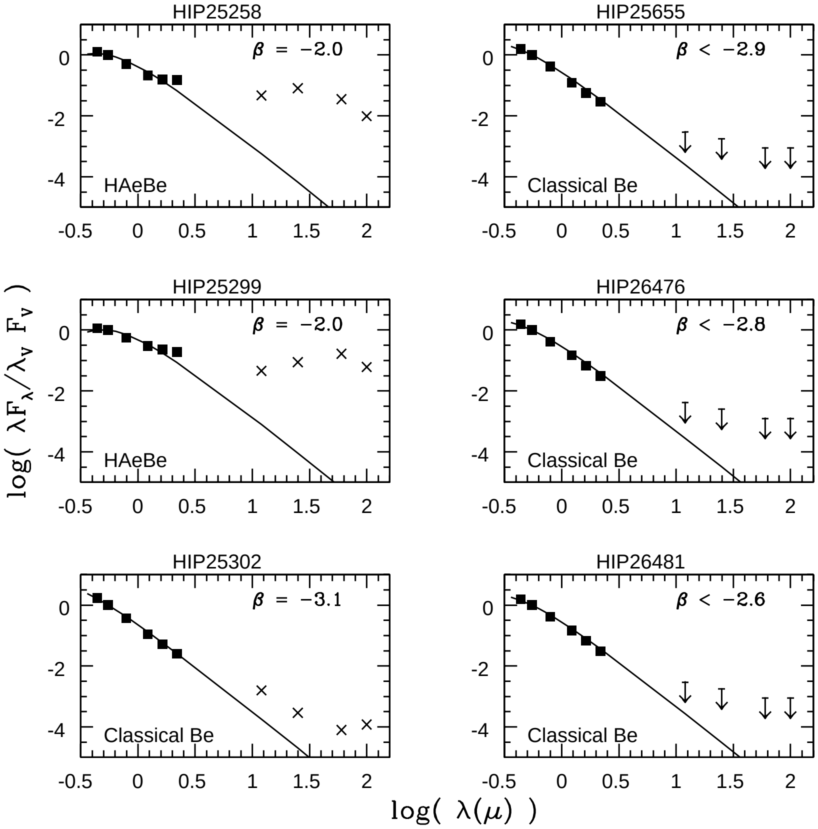

Fig. 7.— SEDs of emission line stars in Ori OB1a. Labels as in Figures 5 and 6.

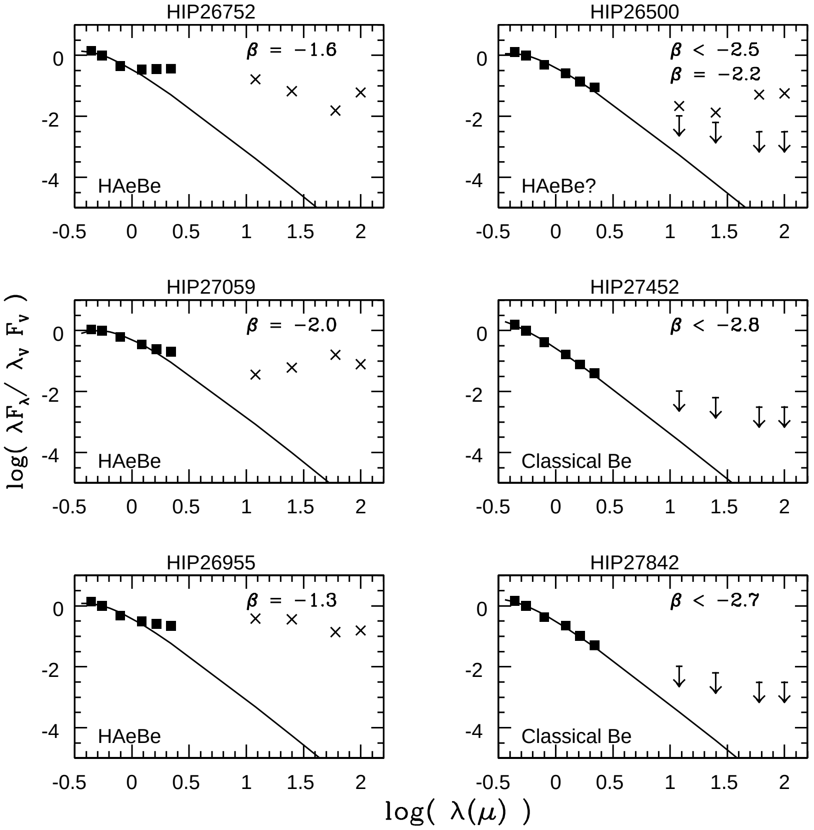

Fig. 8.— SEDs of emission line stars in Ori OB1bc. Labels as in Figures 5 and 6. The three objects on the left column panels show clear evidence to be HAeBe. The status of HIP26500 is uncertain (see §4.5).

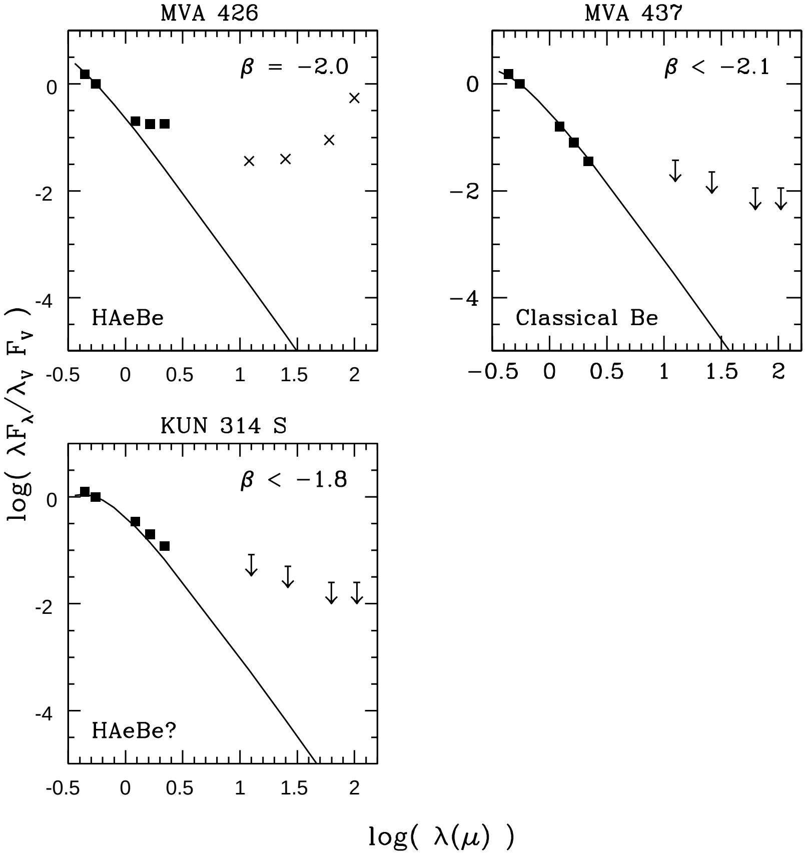

Fig. 9.— SEDs of emission line stars in Trumpler 37. Labels as in Figures 5 and 6. Only the star MVA 426 has IRAS fluxes that confirm its classification as HAeBe. The upper limits in the IRAS fluxes for MVA 437 suggest that this star is not a HAeBe. The status of KUN 314S is uncertain (see §4.6).

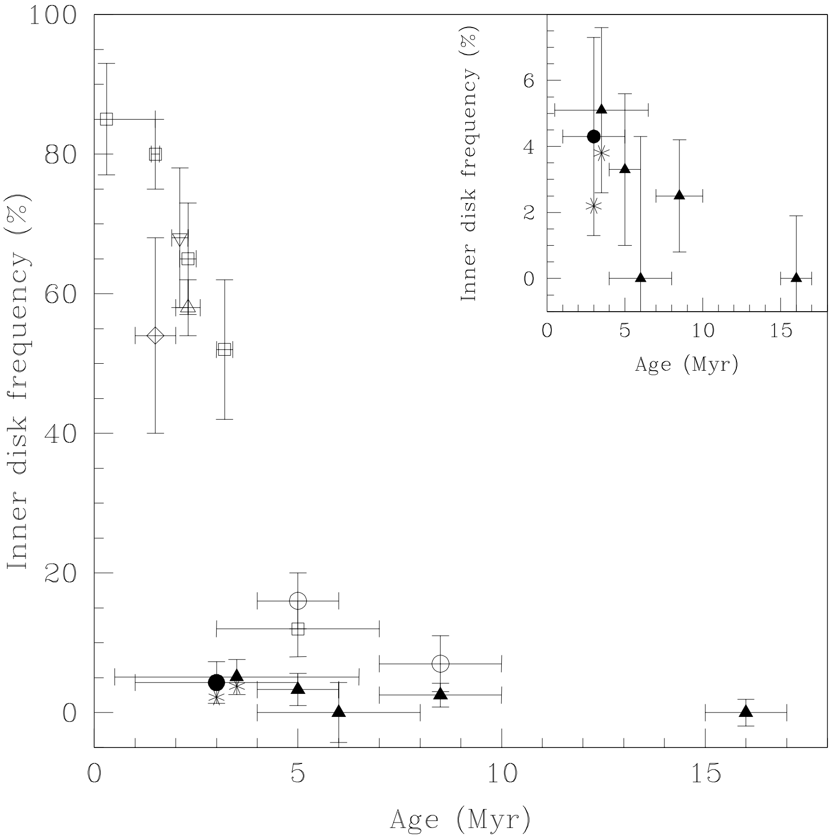

Fig. 10.— Inner Disk frequency as a function of the age of the stellar group. The solid symbols represent the inner disk frequencies for intermediate mass stars estimated from the relative numbers of HAeBe stars in each OB association. From left to right, the solid triangles represent Ori OB1bc (§4.5), Upper Scorpius (§4.1), Per OB2 (§4.2), Ori OB1a (§4.4), and Lac OB1 (§4.3). The solid dot shows the position of Tr 37 (§4.6; Contreras et al. 2002). The asterisks represents the inner disk fractions assuming that the stars HIP26500 (Ori OB1bc) and KUN 314S (Tr 37) are CBe. For comparison, the open symbols represent the disk frequency for the low mass stars, derived using JHKL observations. From left to right, the open squares represent the disks frequency in NGC2024, Trapezium, IC348, NGC2264 and NGC2362 from Haisch, Lada, & Lada (2001). The open triangle and the inverse open triangle show the position on the diagram for Taurus (KH95) and Chameleon I (Gómez & Kenyon 2001). The diamond symbol represents NGC7129 (Gutermuth et al. 2004). The open circles represent our estimates of inner disk frequencies from the sample of Briceño et al. (2004) for Ori OB1a and Ori OB1b using the H-K color (see §4.4 and 4.5). The inner panel shows a zoom of the frequency values calculated for the intermediate mass stars.

arXiv:astro-ph/0410494v1 20 Oct 2004

Table 1. Stellar Properties

Hipparcos	Name	SpT	Error	A_V	$\sigma(A_V)$	J	J-H	$H-K_S$	$\log(T_{\rm eff})$	$\log(L/L_\odot)$	$M/M_\odot$
Upper Scorpius											
HIP76071	HD138343	B9	1	0.28	0.14	7.11	0.03	0.08	4.02	1.64	2.5
HIP76310	HD138813	A1	2	0.09	0.23	7.16	-0.02	0.01	3.96	1.43	2.2
HIP76503	HD139160	B8	1	0.24	0.08	6.17	-0.06	0.04	4.08	2.16	3.4
HIP76633	HD139486	B9	1	0.33	0.14	7.48	-0.01	-0.00	4.02	1.50	2.6
HIP77457	HD141190	A7	2	0.15	0.22	7.41	0.04	0.09	3.89	1.14	1.8
HIP77545	HD141441	A9	2	0.59	0.27	8.14	0.15	0.10	3.87	0.81	1.5
HIP77635	HD141637	B2	1	0.52	0.12	4.80	-0.06	0.08	4.38	3.59	10.3
HIP77813	HD142113	F7	2	0.71	0.15	7.78	0.36	0.12	3.79	0.87	1.6
HIP77840	HD142114	B2	2	0.41	0.20	4.74	-0.07	0.03	4.31	3.41	7.6
HIP77858	HD142165	B6	1	0.37	0.07	5.34	-0.04	0.03	4.15	2.70	4.6
HIP77859	HD142184	B4	2	0.44	0.18	5.44	0.02	0.05	4.25	2.96	5.8
HIP77900	HD142250	B6	1	0.19	0.05	6.23	-0.08	0.01	4.15	2.32	3.9
HIP77909	HD142301	B8	1	0.08	0.08	5.92	-0.07	0.01	4.08	2.23	3.6
HIP77911	HD142315	B9	1	0.34	0.11	6.68	0.02	0.01	4.05	1.88	2.8
HIP77939	HD142378	B4	1	0.50	0.11	5.88	0.02	0.02	4.25	2.77	5.9
HIP77960	HD142424	A8	2	0.41	0.27	7.54	0.07	0.08	3.87	1.07	1.8
HIP78099	HD142705	A1	2	0.52	0.17	7.25	-0.03	0.10	3.96	1.43	2.2
HIP78168	HD142883	B3	1	0.62	0.14	5.76	-0.00	0.03	4.27	2.91	6.7
HIP78207[1]	48 Lib	B1	2	0.62	0.41	5.10	0.27	0.24	4.44	3.66	12.8
HIP78233	HD142989	F4	2	0.41	0.17	7.99	0.18	0.12	3.82	0.81	1.5
HIP78246	HD142990	B2	2	0.39	0.16	5.58	-0.09	0.02	4.34	3.15	8.0
HIP78494	HD143472	F2	2	0.01	0.13	7.07	0.09	0.09	3.84	1.17	1.9
HIP78530	HD143567	B9	1	0.46	0.14	6.93	-0.02	0.04	4.02	1.73	2.6
HIP78549	HD143600	B9	1	0.34	0.14	7.04	-0.00	0.07	4.00	1.59	2.4
HIP78663	HD143811	F5	2	0.23	0.17	7.97	0.19	0.08	3.81	0.81	1.5
HIP78702	HD143956	B9	1	0.47	0.15	7.38	0.04	0.10	4.00	1.46	2.3
HIP78809	HD144175	B9	1	0.44	0.15	7.41	0.04	0.02	4.02	1.54	2.4
HIP78847	HD144254	A1	2	0.44	0.24	7.31	0.09	0.08	3.96	1.38	2.1
HIP78877	HD144334	B9	1	0.01	0.11	6.03	0.06	0.05	4.05	2.13	3.0
HIP78956	HD144569	B9	1	0.82	0.15	7.40	0.09	0.09	4.02	1.60	2.5
HIP78968	HD144586	B9	1	0.68	0.15	7.43	-0.02	0.06	4.00	1.55	2.4
HIP78977	HD144548	F4	2	0.77	0.15	7.54	0.40	0.10	3.81	1.10	1.8
HIP78996	HD144587	A8	2	0.44	0.23	7.47	0.11	0.12	3.87	1.10	1.8
HIP79031	HD144661	B7	1	0.19	0.07	6.38	-0.06	0.00	4.09	2.13	3.3
HIP79054	HD144729	F1	2	0.50	0.16	8.15	0.24	0.08	3.84	0.80	1.6
HIP79083	HD144822	F3	2	0.69	0.12	7.09	0.32	0.10	3.82	1.19	1.9
HIP79097	HD144823	F4	2	0.43	0.12	7.60	0.27	0.07	3.82	0.94	1.6
HIP79098	HD144844	B9	1	0.29	0.11	5.74	-0.01	0.03	4.05	2.26	3.4
HIP79124	HD144925	A0	1	0.86	0.15	7.19	0.16	0.02	4.00	1.62	2.5
HIP79156	HD144981	A0	2	0.74	0.24	7.59	0.01	0.10	3.98	1.42	2.2
HIP79250	HD145189	A4	2	0.30	0.21	7.37	0.05	0.07	3.92	1.29	1.9
HIP79258	HD145132	F3	2	0.29	0.14	8.43	0.20	0.02	3.82	0.66	1.4

Table 1—Continued

Hipparcos	Name	SpT	Error	A_V	$\sigma(A_V)$	J	J-H	H-K_S	log($T_{\rm eff}$)	log($L/L_\odot$)	$M/M_\odot$
HIP79288	HD145263	F0	2	0.47	0.20	8.08	0.13	0.07	3.86	0.86	1.6
HIP79366	HD145468	A5	2	0.64	0.16	7.45	0.08	0.10	3.92	1.25	1.9
HIP79369	HD145467	A8	2	0.80	0.27	7.86	0.20	0.09	3.88	0.99	1.7
HIP79374	HD145502	B2	1	0.97	0.22	3.97	0.17	-0.08	4.38	4.02	11.7
HIP79404	HD145482	B2	1	0.21	0.23	4.98	-0.03	0.03	4.38	3.48	9.8
HIP79410	HD145554	B9	1	0.64	0.15	7.17	0.00	0.10	4.02	1.63	2.5
HIP79439	HD145631	B9	1	0.63	0.15	7.05	0.00	0.11	4.02	1.65	2.5
HIP79476 [1]	V718 Sco	A6	2	0.91	0.24	7.69	0.43	0.57	3.92	1.11	1.8
HIP79530	HD145792	B5	1	0.59	0.11	6.16	0.03	0.04	4.21	2.53	4.9
HIP79599	HD145964	B9	1	0.19	0.14	6.34	-0.05	0.04	4.02	1.94	2.8
HIP79606	HD145998	F2	2	1.25	0.14	7.53	0.29	0.16	3.84	1.11	1.8
HIP79622	HD146001	B8	1	0.36	0.08	5.86	-0.04	0.08	4.08	2.26	3.7
HIP79643	HD146069	F1	2	0.76	0.18	8.36	0.22	0.12	3.85	0.75	1.5
HIP79644	HD146089	F0	2	1.39	0.27	8.90	0.24	0.12	3.86	0.74	1.5
HIP79733	HD146236	F2	2	0.38	0.14	8.16	0.14	0.09	3.84	0.76	1.5
HIP79739	HD146285	B9	1	0.84	0.12	7.24	0.07	0.15	4.05	1.65	2.8
HIP79771	HD146331	B9	1	1.14	0.15	7.33	0.14	0.09	4.02	1.53	2.4
HIP79785	HD146416	B9	1	0.22	0.14	6.51	-0.00	0.03	4.02	1.87	2.8
HIP79860	HD146569	A0	1	0.47	0.15	7.94	0.03	-0.01	4.00	1.27	2.3
HIP79878	HD146606	A0	1	0.00	0.14	7.03	-0.07	0.06	3.98	1.51	2.3
HIP79897	HD146706	B9	1	0.51	0.15	7.08	0.04	0.02	4.00	1.58	2.4
HIP79910	HD146743	F2	2	0.64	0.14	7.84	0.23	0.07	3.83	0.93	1.6
HIP79977	HD146897	F1	2	0.47	0.15	8.06	0.21	0.05	3.84	0.82	1.6
HIP79987	HD146899	A7	2	1.33	0.25	8.57	0.26	0.13	3.90	0.71	1.7
HIP80019	HD147009	B9	1	1.07	0.15	7.25	0.12	0.05	4.02	1.63	2.5
HIP80024	HD147010	A8	2	0.00	0.18	6.75	0.00	0.07	3.88	1.32	2.0
HIP80059	HD147083	A7	2	0.52	0.21	7.77	0.18	0.09	3.90	1.04	1.8
HIP80088	HD147137	A8	2	0.63	0.24	8.03	0.13	0.12	3.88	0.91	1.7
HIP80130	HD147220	A6	2	0.93	0.23	7.62	0.14	0.11	3.92	1.20	1.9
HIP80196	HD147343	A2	2	1.87	0.23	7.57	0.30	0.17	3.95	1.30	2.1
HIP80238	HD147432	A3	2	0.56	0.18	6.85	0.16	0.07	3.94	1.50	2.4
HIP80311	HD147592	A0	1	0.91	0.18	8.15	0.09	0.09	3.97	1.12	2.1
HIP80324	HD147553	A0	1	0.13	0.14	6.96	-0.04	0.02	4.00	1.86	2.7
HIP80338	HD147648	B8	1	2.58	0.12	7.29	0.35	0.22	4.08	1.81	3.1
HIP80371	HD147701	B5	1	2.11	0.08	6.67	0.29	0.19	4.19	2.31	4.3
HIP80425	HD147809	A0	2	1.30	0.24	7.43	0.21	0.16	3.98	1.42	2.2
HIP80461	HD147888	B4	1	1.28	0.07	5.70	0.14	0.12	4.21	2.67	4.8
HIP80473	HD147933	B2	2	1.38	0.17	3.57	0.22	0.17	4.34	3.89	9.6
HIP80474	HD147932	B8	2	1.29	0.12	6.11	0.19	0.15	4.09	2.20	3.4
HIP80493	HD147955	A0	1	0.85	0.14	7.30	0.12	0.10	4.00	1.49	2.3
HIP80569 [1]	HD148184	B5	1	1.10	0.06	3.40	0.26	0.26	4.19	3.56	8.1
HIP80586	HD148153	F5	2	0.21	0.14	7.42	0.15	0.08	3.81	1.08	1.8
HIP80799	HD148562	A4	2	0.15	0.20	7.46	0.06	0.10	3.93	1.22	1.9
HIP80896	HD148716	F3	2	0.19	0.11	7.69	0.14	0.10	3.83	0.94	1.6
HIP81455	HD149790	F5	2	0.18	0.15	8.26	0.21	0.01	3.81	0.69	1.4

Table 1—Continued

Hipparcos	Name	SpT	Error	A_V	$\sigma(A_V)$	J	J-H	H-K_S	log($T_{\rm eff}$)	log($L/L_\odot$)	$M/M_\odot$
HIP81474	HD149914	B9	1	0.95	0.14	5.90	0.11	0.09	4.02	2.11	3.0
HIP81624 [1]	V2307 Oph	A0	2	1.70	0.18	6.95	0.73	0.74	4.00	1.55	2.4
HIP81851	HD150589	F3	2	0.08	0.16	7.69	0.13	0.06	3.82	0.93	1.6
HIP82218	HD151376	F3	2	0.35	0.15	8.06	0.17	0.09	3.83	0.79	1.5
HIP82319	HD151594	F3	2	0.18	0.13	8.05	0.15	0.02	3.83	0.79	1.5
HIP82397	HD151721	A3	2	0.01	0.20	7.32	-0.00	0.02	3.93	1.29	2.1
Perseus OB2											
HIP14145	BD+42 684	F8	1	0.23	0.13	8.60	0.21	0.06	3.79	1.19	2.1
HIP14207	HD18830	A1	2	0.23	0.24	8.08	0.05	0.01	3.96	1.75	2.6
HIP14458	HD19197	B9	1	0.43	0.14	8.76	-0.01	0.04	4.05	1.77	2.7
HIP14552	HD19359	B9	1	0.68	0.14	8.56	0.02	0.01	4.05	1.86	2.8
HIP14713	HD19567	A0	1	0.23	0.14	7.41	-0.04	0.05	4.00	2.11	3.1
HIP14824	HD19664	M5	1	0.00	0.31	2.99	1.01	0.28	3.51	3.21	· · ·
HIP14869	HD19749	A0	1	0.31	0.16	8.93	-0.02	0.03	4.00	1.53	2.4
HIP15601	HD20653	B9	1	0.60	0.12	8.31	0.02	0.03	4.05	1.93	2.8
HIP15696	HD20825	G6	2	1.29	0.15	3.69	0.44	0.15	3.76	3.29	· · ·
HIP15895	HD20987	B2	1	0.50	0.11	8.00	-0.08	-0.05	4.34	2.90	6.9
HIP15984	BD+30 540	B6	3	1.42	0.23	8.34	0.05	0.04	4.13	2.23	3.6
HIP16164	BD+29 564	B9	1	1.06	0.18	8.84	0.10	0.01	4.02	1.67	2.5
HIP16705	HD22125	A0	1	0.64	0.16	8.38	0.03	0.04	3.98	1.70	2.6
HIP16784	HD22281	G4	1	1.93	0.31	6.51	0.60	0.16	3.75	2.16	· · ·
HIP17113	HD278942	B0	2	4.41	0.28	5.88	0.44	0.16	4.48	4.32	14.8
HIP17172	HD22765	A5	2	0.31	0.24	8.83	0.01	0.10	3.91	1.37	2.0
HIP17313	HD22951	B1	1	0.65	0.18	5.00	-0.07	0.01	4.41	4.26	13.4
HIP17474	HD23244	B7	1	0.40	0.08	8.18	0.01	0.01	4.09	2.08	3.1
HIP17498	HD23268	B9	1	0.54	0.15	7.99	-0.00	0.02	4.00	1.99	2.9
HIP17561	HD281157	B1	1	2.68	0.45	7.41	0.17	0.08	4.38	3.26	8.4
HIP17596	HD23427	G8	1	2.10	0.07	5.55	0.75	0.17	3.75	2.68	· · ·
HIP17698	HD23597	B3	1	1.11	0.12	7.99	0.06	0.03	4.25	2.80	5.9
HIP17735	HD23625	B3	1	0.69	0.10	6.37	-0.05	0.00	4.27	3.33	7.2
HIP17845	HD23802	B6	1	1.07	0.19	6.97	0.03	0.01	4.17	2.89	4.9
HIP17998	HD24012	B7	2	0.34	0.12	7.71	-0.12	0.10	4.13	2.35	3.9
HIP18081	HD24131	B1	1	0.69	0.18	5.73	-0.08	0.02	4.41	3.95	11.3
HIP18111	HD24190	B2	1	0.81	0.16	7.26	-0.03	0.03	4.34	3.20	7.9
HIP18246	HD24398	O9	2	1.82	0.25	2.60	-0.02	0.02	4.51	5.85	· · ·
HIP18258	HD281305	B9	2	1.80	0.28	8.24	0.10	0.10	4.02	2.01	2.9
HIP18330	HD24525	G5	2	1.20	0.14	6.24	0.46	0.12	3.76	2.24	· · ·
HIP18392	HD24601	B9	1	0.88	0.12	8.25	0.06	0.02	4.05	2.06	2.9
HIP18397	HD24600	B8	1	0.97	0.12	8.13	0.01	0.01	4.05	2.10	3.0
HIP18578	HD24885	B9	1	0.75	0.16	8.79	-0.01	0.03	4.00	1.68	2.5
HIP18610	HD24913	A0	1	0.72	0.15	7.88	0.01	0.04	4.00	1.98	2.9
HIP18886	HD281486	B9	2	0.74	0.18	9.37	0.01	0.06	4.02	1.46	2.5
HIP19039	HD25539	B2	2	0.68	0.22	6.79	0.03	-0.06	4.34	3.37	8.6

Table 1—Continued

Hipparcos	Name	SpT	Error	A_V	$\sigma(A_V)$	J	J-H	H-K_S	$\log(T_{\rm eff})$	$\log(L/L_\odot)$	$M/M_\odot$
HIP19178	HD25799	B3	2	0.74	0.16	6.88	-0.04	-0.02	4.31	3.24	7.0
HIP19201	HD25833	B4	1	0.47	0.08	6.62	-0.05	-0.02	4.23	3.09	6.1
HIP19240	HD281537	B9	1	0.63	0.14	8.78	0.03	0.03	4.05	1.75	2.7
HIP19659	HD26499	B9	1	0.70	0.16	8.67	0.01	0.04	4.02	1.76	2.6
Lacerta OB1											
HIP106656	HD205742	A0	2	0.13	0.21	8.77	-0.03	0.01	3.98	1.75	2.7
HIP108508	BD+47 3639	B4	1	0.42	0.09	8.66	-0.04	0.01	4.22	2.42	4.5
HIP108841	HD209483	B8	1	0.33	0.08	8.08	-0.01	-0.01	4.07	2.28	3.8
HIP108933	HD209679	A1	2	0.19	0.20	6.29	-0.02	0.04	3.97	2.69	5.3
HIP109082	HD209961	B2	1	0.46	0.14	6.36	-0.13	0.02	4.37	3.81	10.2
HIP110033	BD+40 4771	B9	1	0.45	0.11	9.36	-0.03	0.01	4.05	1.78	2.7
HIP110373	HD212153	B7	1	0.30	0.06	8.36	-0.06	0.00	4.13	2.36	3.9
HIP110473	BD+46 3676	A4	2	0.31	0.23	9.62	0.06	0.04	3.93	1.33	2.2
HIP110476 [1]	BD+42 4370	B7	1	0.60	0.09	8.91	0.04	0.11	4.11	2.06	3.3
HIP110664	HD212668	B4	1	0.37	0.10	8.19	-0.09	0.01	4.24	2.75	5.0
HIP110700	HD212732	B9	1	0.10	0.15	9.45	-0.06	0.00	4.02	1.58	2.5
HIP110790	HD212883	B1	1	0.39	0.16	6.70	-0.14	-0.03	4.41	3.79	10.3
HIP110804	BD+45 3940	A1	3	0.00	0.34	10.12	-0.03	-0.03	3.96	1.08	2.1
HIP110835	BD+43 4205	B9	1	0.22	0.14	9.86	-0.01	-0.00	4.03	1.48	2.5
HIP110849	HD212978	B2	1	0.32	0.14	6.41	-0.13	0.01	4.38	3.81	10.2
HIP110953	HD213190	B5	1	0.28	0.08	9.15	-0.06	-0.00	4.20	2.22	4.2
HIP111038	BD+40 4831	F0	2	0.00	0.23	9.04	0.06	0.04	3.86	1.26	2.0
HIP111080	HD213390	B8	1	0.42	0.09	8.65	0.00	0.00	4.08	2.08	3.3
HIP111104	HD213420	B1	1	0.50	0.16	4.99	0.29	-0.05	4.39	4.56	16.6
HIP111139	HD213484	B7	1	0.31	0.07	8.22	-0.05	0.00	4.10	2.33	3.8
HIP111292	HD213732	A2	3	0.00	0.33	10.01	-0.04	-0.03	3.95	1.07	1.9
HIP111308	BD+36 4868	G0	2	-1.36	0.15	8.66	0.46	0.08	3.78	0.45	1.9
HIP111329	HD213800	B9	1	0.14	0.12	9.14	-0.03	0.03	4.04	1.75	2.7
HIP111337	HD213801	B8	1	0.14	0.08	8.18	-0.05	-0.03	4.06	2.21	3.7
HIP111340	HD213833	A8	2	0.15	0.26	8.69	0.12	0.04	3.88	1.48	2.3
HIP111375	BD+40 4852	B9	1	0.13	0.15	9.94	-0.07	0.02	4.01	1.39	2.4
HIP111429	HD213976	B3	1	0.24	0.12	7.19	-0.08	-0.02	4.29	3.23	7.0
HIP111491	HD214098	B3	1	0.45	0.14	8.42	-0.04	-0.03	4.30	2.82	6.4
HIP111546 [1]	HD214167	B2	2	0.18	0.28	5.78	-0.07	0.15	4.34	3.86	9.4
HIP111552	HD214179	B8	1	0.33	0.10	9.57	-0.02	0.01	4.08	1.72	2.9
HIP111576	HD214243	B3	1	0.25	0.12	8.50	-0.07	-0.02	4.26	2.66	5.5
HIP111589	HD214263	B0	2	0.50	0.19	7.12	-0.11	-0.02	4.46	3.82	13.2
HIP111591	HD214311	B9	1	0.43	0.19	10.18	-0.02	0.02	4.01	1.34	2.3
HIP111683	HD214432	B1	2	0.51	0.20	7.74	-0.09	-0.02	4.43	3.44	10.4
HIP111762	BD+51 3434	K2	1	1.46	0.39	7.26	0.72	0.19	3.69	1.89	···
HIP111814	BD+36 4896	A0	2	0.27	0.22	9.42	0.00	0.01	3.98	1.47	2.3
HIP111916	BD+38 4834	A2	2	0.24	0.21	9.27	0.01	0.03	3.95	1.47	2.3
HIP112016	HD215025	B9	1	0.18	0.13	7.78	-0.02	0.01	4.00	2.21	3.5

Table 1—Continued

Hipparcos	Name	SpT	Error	A_V	$\sigma(A_V)$	J	J-H	$H-K_S$	$\log(T_{\rm eff})$	$\log(L/L_\odot)$	$M/M_\odot$
HIP112017	HD214977	B7	1	0.45	0.06	9.29	0.01	0.00	4.12	2.00	3.4
HIP112031	HD214993	B1	1	0.38	0.16	5.48	-0.10	-0.04	4.41	4.27	13.6
HIP112144	HD215191	B1	1	0.39	0.14	6.61	-0.06	0.00	4.38	3.74	9.8
HIP112148 [1]	HD215227	B0	2	1.20	0.24	8.23	0.10	0.25	4.48	3.38	···
HIP112167	HD215211	B6	1	0.23	0.05	8.73	-0.05	-0.03	4.14	2.21	3.7
HIP112182	HD215271	A2	2	0.16	0.25	10.14	-0.01	0.05	3.95	1.08	2.0
HIP112213	BD+39 4919	A1	2	0.22	0.27	9.54	0.09	0.03	3.96	1.34	2.1
HIP112293	BD+39 4920	B9	1	0.40	0.12	9.71	0.07	0.01	4.03	1.55	2.6
HIP112639	HD216037	B8	1	0.61	0.09	8.75	0.02	0.01	4.07	2.06	3.3
HIP112700	HD216107	B8	1	0.68	0.08	8.13	-0.00	0.03	4.07	2.32	3.9
HIP112710	HD216117	B9	1	0.77	0.16	9.45	0.01	0.01	4.02	1.69	2.6
HIP112805	HD216255	A0	2	0.43	0.20	8.06	-0.03	0.03	3.98	2.10	3.3
HIP112906	BD+38 4883	B9	1	0.20	0.11	9.44	-0.05	0.01	4.03	1.64	2.6
HIP113003	HD216537	B6	1	0.47	0.07	8.63	-0.09	0.04	4.15	2.29	3.8
HIP113110	HD216684	B2	1	0.59	0.15	7.76	-0.11	0.02	4.37	3.26	8.4
HIP113145	HD216733	A5	2	1.16	0.20	6.54	0.17	0.12	3.92	2.52	5.0
HIP113187	HD216797	B8	1	0.54	0.11	8.02	0.00	-0.00	4.07	2.33	3.9
HIP113188	HD216795	B8	1	0.40	0.09	8.64	-0.04	0.01	4.08	2.12	3.3
HIP113208	HD216815	B2	2	0.81	0.20	8.20	-0.02	-0.05	4.34	3.06	7.7
HIP113226 [1]	HD216851	B2	2	0.81	0.20	7.67	0.05	0.16	4.34	3.19	8.0
HIP113281	HD216916	B1	1	0.29	0.14	5.88	-0.13	-0.03	4.38	4.04	11.9
HIP113371	HD217101	B1	1	0.34	0.14	6.46	-0.15	-0.03	4.41	3.88	11.0
HIP113411	HD217161	B9	1	0.65	0.45	9.05	-0.06	0.04	4.04	2.03	2.9
HIP113469	HD217227	B1	1	0.56	0.17	7.25	-0.07	-0.02	4.39	3.54	10.2
HIP113474	HD217262	B3	1	0.82	0.11	7.99	-0.06	-0.02	4.30	3.01	6.9
HIP113731	HD217713	B6	2	0.47	0.08	8.21	-0.02	-0.01	4.15	2.44	4.1
HIP113835	BD+48 3916	B3	1	0.21	0.14	9.64	-0.04	0.01	4.26	2.08	···
HIP113950	BD+43 4383	B9	1	0.23	0.19	9.99	-0.01	0.05	4.04	1.32	2.4
HIP114097	HD218344	B1	1	0.47	0.13	7.63	-0.09	-0.03	4.41	3.43	9.1
HIP114106	HD218326	B4	1	0.36	0.07	8.06	-0.04	-0.06	4.22	2.73	4.9
HIP114134	HD218364	B4	1	0.62	0.10	8.46	-0.07	0.01	4.25	2.69	5.4
HIP114153	BD+45 4144	A0	2	0.55	0.26	9.82	0.04	-0.00	3.98	1.40	2.2
HIP114441	HD218844	B1	1	0.60	0.16	8.24	-0.03	-0.03	4.39	3.13	7.4
HIP114554	HD219016	A6	2	0.27	0.21	8.64	0.07	0.01	3.92	1.63	2.4
HIP114593	BD+47 4075	A0	1	0.37	0.15	9.57	-0.03	0.04	3.99	1.54	2.4
HIP114625	BD+45 4171	A3	2	0.26	0.21	10.17	-0.03	0.03	3.94	1.14	1.9
HIP114890	HD219574	A6	2	0.35	0.21	8.69	0.04	0.06	3.91	1.66	2.5
HIP114909	BD+36 5034	F1	2	0.01	0.20	8.94	0.08	0.07	3.85	1.31	2.0
HIP115067	HD219813	B8	1	0.66	0.11	8.54	-0.03	-0.07	4.07	2.23	3.7
HIP115334	HD220210	B9	1	0.37	0.13	8.21	0.04	0.03	4.04	2.17	3.2
HIP115441	BD+38 4988	A2	2	0.20	0.21	8.68	0.02	0.01	3.95	1.69	2.6
HIP116088	HD221379	A5	3	0.23	0.26	7.81	0.06	0.02	3.91	2.02	3.4
HIP116135	BD+46 4070	A2	2	0.46	0.23	9.47	-0.01	0.07	3.96	1.49	2.3
HIP116540	HD222064	B8	1	0.21	0.09	8.68	-0.04	-0.03	4.08	2.06	3.2

Table 1—Continued

Hipparcos	Name	SpT	Error	A_V	$\sigma(A_V)$	J	J-H	H-K_S	$\log(T_{\rm eff})$	$\log(L/L_\odot)$	$M/M_\odot$
Orion OB1a											
HIP23289	BD-00 819	F1	2	0.00	0.28	9.37	0.19	0.04	3.85	0.84	1.7
HIP23295	HD32056	B9	1	0.37	0.45	8.26	-0.05	0.04	4.00	2.03	2.9
HIP23313	HD32114	B9	1	0.27	0.18	9.42	-0.01	0.03	4.00	1.43	2.3
HIP23434	BD-01 779	G6	2	1.01	0.18	7.30	0.53	0.10	3.76	1.78	3.9
HIP23441	BD-01 781	F1	2	0.50	0.37	10.22	0.17	0.03	3.85	0.83	1.6
HIP23469	HD32350	A7	2	0.00	0.24	8.91	0.08	0.03	3.90	1.20	1.9
HIP23473	HD32359	B7	1	0.07	0.05	7.51	-0.10	0.03	4.12	2.48	4.1
HIP23514	HD32465	B9	1	0.00	0.13	8.38	-0.02	-0.01	4.02	1.83	2.7
HIP23515	HD289883	A1	2	0.20	0.31	10.05	0.00	0.03	3.96	1.05	2.0
HIP23643	HD32686	B5	1	0.08	0.05	6.26	-0.05	-0.04	4.20	3.18	6.1
HIP23654	HD32663	A1	2	0.00	0.23	8.57	-0.06	0.00	3.96	1.58	2.4
HIP23659	HD32720	A0	1	0.12	0.15	9.01	0.03	0.05	4.00	1.52	2.4
HIP23700	HD287493	G1	2	0.73	0.17	7.96	0.48	0.12	3.77	1.51	2.9
HIP23714	HD32816	A0	1	0.16	0.14	8.11	-0.04	0.01	4.00	1.92	2.8
HIP23757	HD32867	B8	1	0.00	0.09	7.69	-0.07	-0.05	4.08	2.27	3.7
HIP23837	HD33056	B9	1	0.06	0.14	8.82	-0.05	0.08	4.01	1.62	2.5
HIP23846	HD33037	B9	1	0.09	0.11	8.04	-0.07	0.03	4.03	2.03	2.9
HIP23899	HD33110	A3	2	0.00	0.18	7.00	0.00	0.06	3.94	2.13	3.5
HIP23907	HD287545	G1	2	1.53	0.18	7.28	0.57	0.09	3.77	1.96	4.2
HIP23919	HD33190	B8	1	0.05	0.07	8.35	-0.06	-0.04	4.09	2.02	3.1
HIP24048	HD33403	B9	1	0.13	0.14	8.24	-0.03	0.06	4.00	1.85	2.7
HIP24127	HD33546	B9	1	0.25	0.13	7.72	-0.04	0.02	4.01	2.09	3.0
HIP24297	HD33819	B9	1	0.17	0.18	9.30	-0.00	0.07	4.01	1.42	2.4
HIP24342	HD33917	A2	2	0.10	0.23	8.94	0.04	0.09	3.96	1.36	2.1
HIP24363	HD33900	B9	1	0.26	0.18	8.61	-0.01	0.06	4.01	1.76	2.6
HIP24367	HD33928	B4	2	0.07	0.11	7.31	-0.05	-0.05	4.22	2.81	5.0
HIP24442	HD34035	A1	2	0.04	0.26	9.09	0.00	0.02	3.97	1.38	2.1
HIP24467	HD34098	B1	1	0.29	0.17	9.03	-0.12	-0.01	4.38	2.59	···
HIP24531	HD34238	A8	2	0.20	0.26	8.19	0.05	0.09	3.88	1.57	2.4
HIP24547	HD34226	A3	2	0.24	0.19	8.25	0.02	0.06	3.94	1.69	2.6
HIP24611	HD34341	B9	1	0.47	0.14	8.42	0.09	-0.02	4.00	1.86	2.8
HIP24635	HD34430	B9	1	0.52	0.13	8.89	-0.02	0.04	4.03	1.75	2.6
HIP24709	HD34511	B6	1	0.05	0.08	7.64	-0.06	-0.04	4.16	2.54	4.3
HIP24747	HD34582	A5	2	0.38	0.20	8.08	0.07	0.07	3.92	1.68	2.5
HIP24757	HD34561	A2	2	0.00	0.25	9.45	-0.01	0.03	3.95	1.12	1.9
HIP24758	HD34595	B9	1	0.34	0.17	9.22	-0.04	0.03	4.02	1.55	2.4
HIP24803	HD34637	A0	1	0.07	0.17	9.38	0.02	0.05	3.99	1.35	2.2
HIP24811	HD34672	B9	1	0.26	0.10	8.40	0.01	0.05	4.05	1.91	2.8
HIP24847	HD34748	B2	1	0.37	0.15	6.57	-0.03	-0.07	4.35	3.52	8.3
HIP24848	HD287738	F7	2	0.05	0.23	8.88	0.33	0.03	3.80	1.07	1.9
HIP24849	HD34747	B9	1	0.35	0.16	8.31	0.03	0.04	4.02	1.86	2.7
HIP24851	HD290240	A0	1	0.13	0.14	9.02	-0.04	0.07	4.00	1.49	2.3
HIP24922	HD34859	B9	1	0.65	0.15	8.55	0.02	0.03	4.03	1.77	2.7

Table 1—Continued

Hipparcos	Name	SpT	Error	A_V	$\sigma(A_V)$	J	J-H	H-K_S	$\log(T_{\rm eff})$	$\log(L/L_\odot)$	$M/M_\odot$
HIP24970	HD34908	A4	2	0.05	0.20	8.92	0.02	0.07	3.92	1.38	2.0
HIP24989	HD34929	B8	1	0.20	0.09	8.39	-0.03	0.00	4.06	1.96	3.1
HIP25025	HD35008	B9	1	0.00	0.13	7.23	-0.09	0.05	4.02	2.28	3.7
HIP25028	HD35007	B3	1	0.22	0.12	5.95	-0.07	-0.03	4.29	3.58	8.2
HIP25044	HD35039	B1	1	0.27	0.15	5.46	0.23	0.02	4.40	4.24	13.3
HIP25121	HD35153	A1	2	0.21	0.17	8.74	-0.05	0.04	3.96	1.52	2.3
HIP25128	HD35135	B9	1	0.15	0.18	8.30	-0.01	0.02	4.02	1.88	2.8
HIP25142	HD35149	B2	2	0.39	0.20	5.35	-0.10	-0.03	4.35	4.07	11.4
HIP25145	HD35148	B4	1	0.15	0.09	7.35	-0.11	-0.02	4.23	2.83	5.0
HIP25152	HD35195	A0	1	0.33	0.15	8.92	0.01	0.02	3.99	1.57	2.4
HIP25163	HD35177	B8	1	0.07	0.08	8.27	-0.05	-0.07	4.08	2.06	3.2
HIP25179	HD35203	B7	1	0.10	0.10	8.08	-0.03	-0.03	4.11	2.20	3.6
HIP25193	HD290385	B9	1	0.17	0.11	8.42	-0.06	-0.02	4.05	1.95	2.9
HIP25199	HD35271	B9	1	0.18	0.12	7.91	-0.05	-0.01	4.03	2.11	3.0
HIP25223	HD35299	B1	1	0.12	0.15	6.13	-0.11	-0.04	4.39	3.77	9.9
HIP25235	HD35298	B9	1	0.00	0.18	8.12	-0.05	-0.10	4.03	1.94	2.9
HIP25241	HD35305	B8	1	0.05	0.08	8.49	-0.11	0.02	4.07	1.92	3.0
HIP25244	HD35318	A3	2	0.31	0.21	9.22	0.01	0.05	3.94	1.35	2.1
HIP25258 [1]	HD287823	A3	2	0.45	0.23	9.24	0.50	0.83	3.94	1.32	2.1
HIP25288	HD35407	B4	1	0.09	0.10	6.60	-0.07	-0.06	4.25	3.19	6.7
HIP25299 [1]	V346 Ori	A8	2	0.00	0.42	9.70	0.51	0.63	3.88	0.88	1.7
HIP25302 [1]	V1086 Ori	B2	1	0.10	0.16	5.37	-0.05	0.06	4.36	4.02	11.3
HIP25327	HD35502	B6	1	0.26	0.06	7.39	-0.03	-0.01	4.14	2.58	4.4
HIP25340	HD35501	B8	1	0.14	0.09	7.53	-0.06	0.02	4.08	2.37	3.9
HIP25368	HD35575	B2	2	0.22	0.17	6.79	-0.03	-0.06	4.36	3.45	9.0
HIP25378	HD35588	B2	1	0.09	0.15	6.53	-0.06	-0.00	4.32	3.39	7.6
HIP25394	HD294046	B9	1	0.00	0.12	8.40	-0.06	-0.03	4.04	1.86	2.8
HIP25411	HD35612	B9	1	0.02	0.12	8.39	-0.02	0.02	4.03	1.87	2.8
HIP25469	HD35716	B9	1	0.02	0.13	8.60	-0.04	-0.02	4.02	1.76	2.6
HIP25473	HD35715	B1	1	0.15	0.16	5.08	-0.11	-0.01	4.39	4.22	13.1
HIP25477	HD35730	B4	1	0.10	0.09	7.51	-0.11	0.00	4.25	2.83	5.1
HIP25480	HD35777	B1	1	0.26	0.13	6.96	-0.15	0.01	4.39	3.45	9.4
HIP25493	HD35762	B2	1	0.24	0.15	7.08	-0.13	0.05	4.36	3.34	8.6
HIP25496	HD35792	B3	1	0.15	0.10	7.49	-0.15	0.00	4.27	2.91	6.4
HIP25507	HD35773	A0	2	0.07	0.29	9.75	-0.01	-0.06	3.98	1.17	2.2
HIP25511	HD35790	B9	1	0.31	0.15	9.14	-0.01	0.00	4.00	1.57	2.4
HIP25533	HD35834	B8	1	0.21	0.07	7.64	-0.03	0.00	4.09	2.31	3.7
HIP25552	HD35882	B6	1	0.14	0.06	7.87	-0.05	0.04	4.13	2.34	3.9
HIP25557	HD35899	B4	1	0.06	0.08	7.78	-0.08	-0.05	4.22	2.63	5.0
HIP25567	HD35881	B7	1	0.10	0.06	7.93	-0.10	-0.03	4.13	2.32	3.8
HIP25582	HD35912	B2	1	0.16	0.10	6.74	-0.09	-0.04	4.35	3.41	8.5
HIP25591	HD244042	A6	2	0.01	0.22	9.02	0.17	0.03	3.92	1.23	1.9
HIP25592	HD35926	B8	1	0.02	0.08	8.41	0.03	-0.11	4.07	1.93	3.0
HIP25594	HD35948	A1	2	0.06	0.20	8.24	0.04	0.01	3.97	1.74	2.6
HIP25595	HD35911	F1	2	0.03	0.18	8.35	0.15	0.09	3.85	1.37	2.1

Table 1—Continued

Hipparcos	Name	SpT	Error	A_V	$\sigma(A_V)$	J	J-H	H-K_S	$\log(T_{\rm eff})$	$\log(L/L_\odot)$	$M/M_\odot$
HIP25600	HD35957	B8	1	0.06	0.08	8.65	-0.03	-0.02	4.08	1.90	2.9
HIP25648	HD36013	B4	1	0.03	0.08	7.19	-0.10	-0.02	4.23	2.88	5.3
HIP25655 [1]	V1372 Ori	B6	1	0.18	0.06	7.44	-0.06	0.12	4.17	2.71	4.6
HIP25725	HD36115	B8	1	0.34	0.08	8.06	-0.01	0.01	4.09	2.15	3.4
HIP25751	HD36166	B1	1	0.18	0.14	6.17	-0.14	-0.02	4.39	3.77	10.0
HIP25752	HD36165	B8	1	0.00	0.09	8.29	-0.11	-0.03	4.09	2.05	3.1
HIP25762	HD36219	B8	1	0.12	0.07	7.74	-0.09	0.02	4.08	2.26	3.7
HIP25828	HD36311	A2	2	0.10	0.23	8.68	-0.03	0.04	3.96	1.66	2.5
HIP25831	HD244459	A8	2	0.14	0.32	9.64	0.04	0.05	3.88	0.98	1.7
HIP25850	HD36340	B1	1	0.35	0.13	8.28	-0.13	-0.03	4.40	2.97	···
HIP25861	HD36351	B2	1	0.15	0.15	5.82	-0.14	-0.02	4.35	3.78	9.0
HIP25881	HD36392	B3	1	0.16	0.12	7.76	-0.13	-0.05	4.26	2.75	5.9
HIP25897	HD36429	B6	1	0.01	0.06	7.74	-0.08	0.00	4.14	2.40	4.0
HIP25979	HD36549	B9	1	0.00	0.13	8.70	-0.03	-0.01	4.02	1.70	2.6
HIP26024	HD36627	B6	1	0.10	0.06	7.78	-0.08	0.02	4.16	2.48	4.2
HIP26045	HD36645	B9	1	0.15	0.14	8.58	-0.04	0.06	4.01	1.74	2.6
HIP26055	HD36654	A0	1	0.19	0.16	9.07	-0.00	0.04	4.00	1.57	2.4
HIP26098	HD36741	B1	1	0.23	0.12	7.00	-0.13	0.03	4.39	3.45	9.3
HIP26143	HD36810	B9	1	0.08	0.13	8.67	-0.02	0.02	4.00	1.71	2.6
HIP26331	HD245519	A6	2	0.23	0.23	9.31	0.07	0.01	3.91	1.26	1.9
HIP26353	HD288063	F4	2	0.00	0.21	8.24	0.11	0.06	3.82	1.46	2.5
HIP26467	HD288112	F3	2	0.00	0.18	8.59	0.10	0.09	3.83	1.29	2.2
HIP26476 [1]	HD37330	B6	1	0.13	0.06	7.63	-0.04	-0.01	4.13	2.47	4.1
HIP26481 [1]	HD37342	B6	1	0.00	0.06	8.26	-0.08	-0.03	4.15	2.23	3.7
HIP26637	HD37592	A0	1	0.00	0.13	8.38	-0.07	0.01	4.00	1.72	2.7
HIP26687	HD37659	A0	2	0.31	0.20	8.63	-0.02	0.06	3.98	1.65	2.5
Orion OB1bc											
HIP23470	HD32394	F1	2	0.07	0.20	8.12	0.15	0.06	3.84	1.71	2.9
HIP24117	HD33547	B9	1	0.05	0.13	8.49	-0.06	-0.03	4.04	2.09	3.0
HIP24458	HD34120	B8	1	0.69	0.15	9.12	0.01	0.07	4.05	1.97	3.1
HIP24466	HD34164	B9	2	0.56	0.21	9.18	0.02	0.13	4.02	1.84	2.7
HIP24556	HD34271	A2	4	0.56	0.36	9.12	0.05	0.04	3.95	1.68	2.6
HIP24596	HD34342	B8	3	0.57	0.26	8.62	0.02	0.05	4.08	2.20	3.5
HIP24701	HD34523	B9	2	0.42	0.20	9.28	0.05	0.04	4.01	1.74	2.6
HIP24752	HD293988	F6	2	0.22	0.24	9.10	0.20	0.04	3.80	1.34	2.3
HIP24891	HD34835	B7	1	0.18	0.10	8.23	-0.05	0.02	4.11	2.41	4.0
HIP24930	HD34890	B9	1	0.47	0.16	8.42	0.21	0.19	4.03	2.04	2.9
HIP24936	HD34889	B9	1	0.01	0.16	8.78	-0.09	0.04	4.02	1.91	2.8
HIP25427	HD35658	A3	2	0.07	0.21	8.67	0.01	0.11	3.94	1.71	2.6
HIP25457	HD294145	F0	3	0.15	0.24	9.39	0.13	0.03	3.86	1.31	2.0
HIP25548	HD35867	B9	1	0.03	0.15	8.24	-0.05	0.04	4.04	2.19	3.2
HIP25643	HD36032	B9	1	0.11	0.16	9.16	-0.05	0.02	4.03	1.80	2.7
HIP25664	HD36046	B8	1	0.00	0.12	8.17	-0.01	-0.03	4.08	2.32	3.8

Table 1—Continued

Hipparcos	Name	SpT	Error	A_V	$\sigma(A_V)$	J	J-H	H-K_S	log($T_{\rm eff}$)	log($L/L_\odot$)	$M/M_\odot$
HIP25691	HD36120	B9	1	0.08	0.15	8.03	-0.06	0.00	4.03	2.28	3.5
HIP25770	HD36234	B9	1	0.03	0.14	8.78	-0.05	-0.03	4.04	2.00	2.9
HIP25804	HD36324	B8	2	0.50	0.14	8.82	0.04	-0.04	4.08	2.13	3.3
HIP25818	HD36312	B8	1	0.10	0.10	8.22	-0.04	-0.01	4.08	2.31	3.8
HIP25849	HD36363	F5	2	0.26	0.20	8.51	0.22	0.04	3.81	1.56	2.8
HIP25863	HD36412	F1	3	1.31	0.24	7.82	0.27	0.14	3.85	1.98	3.6
HIP25870	HD36394	A1	2	0.20	0.27	8.38	-0.02	-0.05	3.97	2.15	3.4
HIP25954	HD36540	B8	1	0.43	0.12	7.86	0.03	0.02	4.08	2.44	4.1
HIP25956	HD36527	A4	3	0.12	0.20	9.16	0.08	0.03	3.93	1.53	2.4
HIP25980	HD36591	B1	2	0.25	0.18	5.74	-0.12	-0.02	4.42	4.28	13.6
HIP25992	HD36617	A0	1	0.14	0.16	8.34	-0.06	0.08	3.99	2.04	3.0
HIP26012	HD36628	B9	1	0.07	0.16	8.01	-0.00	-0.04	4.02	2.24	3.4
HIP26016	BD-01 939C	B9	1	0.00	1.53	8.52	0.02	0.03	4.00	1.93	2.8
HIP26020	HD36646	B3	1	0.24	0.12	6.72	-0.12	0.04	4.26	3.42	7.6
HIP26021	HD36655	B8	3	0.19	0.25	8.59	0.00	0.00	4.09	2.20	3.4
HIP26048	HD36668	B9	1	0.00	0.17	8.20	-0.10	0.01	4.03	2.20	3.2
HIP26063	HD36695	B2	2	0.20	0.23	5.75	-0.06	-0.05	4.38	4.15	12.5
HIP26082	HD36709	B9	1	0.05	0.16	8.36	-0.03	-0.01	4.02	2.09	3.0
HIP26106	HD36779	B2	2	0.16	0.18	6.58	-0.05	-0.07	4.32	3.66	8.5
HIP26120	HD36827	B2	2	0.18	0.22	6.94	-0.11	-0.02	4.34	3.52	8.1
HIP26132	HD36776	B7	1	0.14	0.09	8.64	-0.06	0.03	4.10	2.22	3.6
HIP26136	HD36797	A1	2	0.11	0.49	8.14	0.00	0.06	3.97	2.04	3.0
HIP26188	HD36898	B7	1	0.09	0.07	7.29	-0.12	0.03	4.12	2.80	4.8
HIP26210	HD36935	B6	1	0.05	0.08	7.76	-0.07	-0.02	4.15	2.71	4.6
HIP26213	HD36954	B3	1	0.24	0.12	7.12	-0.03	0.01	4.26	3.27	7.0
HIP26216	HD36997	B9	1	0.06	0.16	8.32	-0.07	0.01	4.04	2.12	3.0
HIP26233	HD37017	B0	1	0.49	0.16	6.80	-0.08	-0.03	4.48	4.03	14.6
HIP26234	HD37016	B4	1	0.03	0.10	6.48	-0.09	-0.02	4.23	3.39	7.4
HIP26257	HD37040	B2	2	0.18	0.19	6.65	-0.09	-0.03	4.34	3.57	8.3
HIP26263	HD37055	B3	1	0.18	0.11	6.59	-0.13	0.00	4.26	3.46	7.7
HIP26265	HD37057	A0	1	0.14	0.16	9.11	0.08	0.03	4.00	1.70	2.6
HIP26271	HD37056	B9	1	0.05	0.13	8.44	-0.00	0.03	4.05	2.14	3.0
HIP26312	HD37141	B9	1	0.23	0.17	8.40	-0.05	0.01	4.03	2.13	3.0
HIP26319	HD37149	B6	1	0.10	0.07	8.16	-0.14	0.00	4.14	2.50	4.2
HIP26405	HD37272	B5	1	0.15	0.09	8.04	-0.06	0.07	4.21	2.74	4.9
HIP26427	HD37303	B1	3	0.14	0.28	6.49	-0.17	-0.00	4.40	3.91	11.0
HIP26431	HD37294	B8	1	0.05	0.09	8.47	-0.11	0.02	4.08	2.22	3.5
HIP26439	HD37321	B5	1	0.15	0.07	7.28	0.03	0.01	4.20	3.02	5.2
HIP26442	HD37334	B2	2	0.22	0.19	7.46	-0.04	-0.04	4.36	3.41	8.9
HIP26456	HD37333	A4	3	0.00	0.21	8.41	-0.07	0.07	3.93	1.86	2.8
HIP26464	HD37332	B4	1	0.10	0.10	7.91	-0.05	-0.05	4.23	2.87	5.2
HIP26477	HD37356	B1	2	0.68	0.20	6.20	-0.03	0.01	4.39	4.05	11.8
HIP26494	HD37370	B7	1	0.28	0.08	7.47	-0.07	0.03	4.13	2.78	4.7
HIP26500 [1]	HD37371	A2	2	0.23	0.22	8.04	0.15	0.35	3.95	1.95	2.9
HIP26508	HD37397	B2	3	0.18	0.26	7.16	-0.06	-0.03	4.32	3.43	7.8

Table 1—Continued

Hipparcos	Name	SpT	Error	A_V	$\sigma(A_V)$	J	J-H	H-K_S	$\log(T_{\rm eff})$	$\log(L/L_\odot)$	$M/M_\odot$
HIP26526	HD37427	B8	1	0.19	0.12	8.70	-0.00	-0.01	4.07	2.15	3.4
HIP26551	HD37468D	B2	2	0.12	0.21	7.12	-0.10	-0.04	4.34	3.47	8.0
HIP26558	HD37480	B9	1	0.16	0.17	9.11	0.03	0.07	4.01	1.76	2.6
HIP26579	HD37525	B5	1	0.18	0.07	8.13	0.03	0.01	4.18	2.62	4.5
HIP26581	HD37526	B5	1	0.08	0.09	7.83	-0.04	-0.03	4.20	2.81	4.8
HIP26644	HD37591	B9	1	0.08	0.15	8.07	-0.05	0.03	4.03	2.26	3.4
HIP26656	HD37642	B9	1	0.00	0.19	8.17	-0.04	0.01	4.02	2.19	3.3
HIP26683	HD37674	B1	2	0.56	0.20	7.72	-0.04	-0.03	4.40	3.42	9.7
HIP26695	HD288174	G3	2	1.82	0.16	6.82	0.53	0.19	3.77	2.41	···
HIP26697	HD37700	B7	1	0.09	0.07	8.26	-0.06	0.01	4.13	2.46	4.1
HIP26713	HD37744	B2	2	0.13	0.19	6.63	-0.10	-0.06	4.37	3.76	9.7
HIP26716	HD37745	A0	1	0.17	0.15	9.12	-0.02	0.03	4.00	1.76	2.6
HIP26736	HD37756	B1	2	0.16	0.18	5.38	-0.13	-0.04	4.39	4.32	13.8
HIP26742	HD37776	B1	1	0.34	0.14	7.29	-0.14	0.01	4.39	3.58	10.0
HIP26752 [1]	HD37806	B9	1	0.21	0.18	7.12	0.86	0.85	4.01	2.29	3.6
HIP26766	HD37807	B3	1	0.25	0.13	8.12	-0.08	-0.03	4.27	2.91	6.4
HIP26816	HD37903	B1	2	1.00	0.19	7.37	-0.05	0.14	4.39	3.52	10.1
HIP26870	HD37958	B9	2	0.12	0.20	6.64	-0.04	0.01	4.04	2.83	5.2
HIP26908	HD38051	B2	1	1.70	0.14	7.65	-0.00	0.11	4.37	3.48	9.2
HIP26914	HD38013	B8	1	0.77	0.17	9.14	0.01	0.06	4.06	1.96	3.1
HIP26934	HD38088	A0	1	0.60	0.18	9.16	0.06	0.03	4.00	1.73	2.6
HIP26955 [1]	HD38120	A0	2	0.13	0.26	8.43	0.58	0.69	3.98	1.74	2.6
HIP27007	HD38165	B7	1	1.12	0.14	8.20	0.05	0.07	4.10	2.52	4.2
HIP27056	HD38249	F2	3	0.00	0.28	8.26	0.10	0.04	3.84	1.71	2.9
HIP27059 [1]	V351 Ori	A9	3	0.37	0.27	7.95	0.45	0.66	3.87	1.83	3.0
HIP27101	HD38311	A0	2	0.16	0.22	8.61	0.01	-0.00	3.98	1.89	2.8
HIP27138	HD38389	A3	3	0.00	0.26	9.87	0.04	0.07	3.94	1.16	1.9
HIP27226	HD38506	A0	2	0.17	0.22	9.43	-0.03	0.08	3.98	1.60	2.5
HIP27258	HD38547	B9	2	0.14	0.20	8.19	0.08	0.03	4.04	2.20	3.2
HIP27261	HD38528	A0	1	0.80	0.16	7.13	0.07	0.08	4.00	2.56	4.5
HIP27452 [1]	HD38856	B5	1	0.03	0.08	7.35	-0.03	0.11	4.18	2.89	4.9
HIP27487	HD38912	B9	1	0.89	0.22	8.88	0.08	0.03	4.02	1.97	2.9
HIP27510	HD39000	B8	1	0.10	0.10	7.66	-0.07	-0.01	4.08	2.52	4.2
HIP27536	HD39034	A0	1	0.17	0.19	9.33	0.03	0.00	4.00	1.69	2.6
HIP27561	HD39067	A5	3	0.06	0.23	8.70	0.07	0.00	3.92	1.71	2.6
HIP27573	HD39082	A2	2	0.00	0.27	7.35	-0.06	0.02	3.96	2.33	4.0
HIP27574	HD39103	A0	1	0.15	0.17	8.96	-0.06	0.04	3.99	1.76	2.6
HIP27580	HD39161	A2	2	0.10	0.24	8.79	0.06	0.05	3.95	1.74	2.6
HIP27645	HD39254	B9	1	1.18	0.19	8.74	0.14	0.05	4.03	2.06	2.9
HIP27744	HD39401	A4	3	0.20	0.22	8.55	-0.00	0.06	3.93	1.82	2.8
HIP27842 [1]	HD39557	B8	1	1.57	0.15	7.76	0.13	0.15	4.08	2.52	4.3
HIP27929	HD39777	B1	2	0.24	0.17	6.90	-0.12	-0.01	4.39	3.72	9.6
HIP28056	HD39953	A0	2	0.31	0.22	6.90	0.01	0.07	3.98	2.58	4.7
HIP28109	HD40067	A1	2	0.10	0.28	8.52	-0.04	0.06	3.96	1.81	2.7
HIP28140	HD40134	A5	3	0.05	0.23	8.37	0.04	0.01	3.92	1.80	2.7

Table 1—Continued

Hipparcos	Name	SpT	Error	A_V	$\sigma(A_V)$	J	J-H	H-K_S	log($T_{\rm eff}$)	log($L/L_\odot$)	$M/M_\odot$
HIP28158	HD40145	F4	2	0.00	0.20	7.67	0.07	0.11	3.82	1.91	3.6
HIP28285	HD40429	B9	2	0.16	0.20	8.49	-0.07	0.01	4.02	2.06	3.0
HIP28334	HD40534	B9	1	0.26	0.14	8.92	-0.07	0.05	4.05	1.95	2.8
HIP28367	HD40575	A0	1	0.23	0.19	9.43	0.00	0.02	3.99	1.64	2.5
HIP28370	HD40574	B7	1	0.14	0.10	6.66	-0.08	0.04	4.11	3.00	5.6

[1] Stars with emission in Hα line (see table 3)